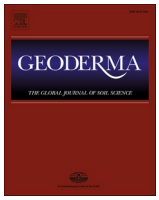
Geoderma 475 (2026) 118113



Contents lists available at ScienceDirect

Geoderma

journal homepage: www.elsevier.com/locate/geoderma



Characteristics of annual CO_2 and N_2O emissions and soil NO_3^- leaching from different urban greenspace landscapes in Denmark

Xiao Bai [a], Tom Cripps [a], Arezoo Taghizadeh-Toosi [b], Shuoyue Wang [a], Klaus Butterbach-Bahl [a,c], Zhisheng Yao [a,d,e,*]

[a] Pioneer Center Land-CRAFT, Department of Agroecology, Aarhus University, Aarhus 8000, Denmark
[b] Danish Technological Institute, Aarhus 8200, Denmark
[c] Institute for Meteorology and Climate Research, Atmospheric Environmental Research, Karlsruhe Institute of Technology, Garmisch-Partenkirchen 82467, Germany
[d] State Key Laboratory of Atmospheric Environment and Extreme Meteorology, Institute of Atmospheric Physics, Chinese Academy of Sciences, Beijing 100029, PR China
[e] College of Earth and Planetary Science, University of Chinese Academy of Sciences, Beijing 100049, PR China

ARTICLE INFO

Handling Editor: Jan Willem Van Groenigen

Keywords:
Nitrous oxide
Urban greenspace
Greenhouse gas emission
Nitrate leaching
Urbanization

ABSTRACT

Urban greenspace landscapes are becoming increasingly common as a result of rapid global urbanization. However, the extent to which soil carbon (C) and nitrogen (N) dynamics differ between these urban greenspaces remains poorly understood. This study reports on a field campaign conducted at the city level in Denmark. During the campaign, we conducted year-round measurements of soil carbon dioxide (CO_2) and nitrous oxide (N_2O) fluxes, as well as soil nitrate (NO_3^-) leaching in five types of urban greenspace: sports fields, roadside patches, residential lawns, urban parks and urban forests. Our results show that the temporal variability in soil N_2O emissions was controlled by the synergistic changes in soil water content and temperature, though neither factor had a strong individual effect. However, soil temperature overrode the effects of soil water content, emerging as the primary factor triggering temporal variations in soil CO_2 fluxes, with temperature sensitivity (Q_{10}) values varying from 2.88 to 3.65. We estimated cumulative annual N_2O and CO_2 emissions for all urban greenspaces to be 0.67–4.08 kg N ha^{-1} yr^{-1} and 12.0–21.2 Mg C ha^{-1} yr^{-1}, respectively. Non-growing season emissions contributed 8.4–48.1% for N_2O and 12.8–21.0% for CO_2 to these annual budgets. Annual soil NO_3^- leaching rates for the studied greenspace ecosystems ranged from 1.2 to 11.8 kg N ha^{-1} yr^{-1}. Of the five greenspace landscapes, sports fields exhibited the highest annual losses of soil N_2O and NO_3^- leaching, while significantly lower values were observed in urban parks and forests. These differences in soil N losses between greenspace types are driven by variations in soil water content and soil NO_3^- availability. Cumulative annual CO_2 emissions across all greenspace landscapes were positively correlated with annual N_2O emissions. At the city scale, the average annual N_2O and CO_2 emissions and soil NO_3^- leaching, weighted by the areal extent of the different urban greenspace types, were estimated at 1.35 kg N ha^{-1} yr^{-1} (N_2O), 17.2 Mg C ha^{-1} yr^{-1} (CO_2) and 2.44 kg N ha^{-1} yr^{-1} (NO_3^- leaching), respectively. Overall, our findings offer valuable insights for better predicting the potential role of urban greenspace ecosystems in regional greenhouse gas and N loss budgets.

1. Introduction

Urbanization is increasing rapidly in most regions of the world and is expected to continue over the next few decades. By 2030, it is projected that up to 60% of the global population will live in urban areas, and the global urban land area will triple compared to the beginning of the 21st century (Seto et al., 2012; United Nations, 2014). The urban sprawl and increasing population densities are associated with development and construction processes, as well as the extensive establishment of various greenspace landscapes such as public parks, residential lawns, urban forests and sports fields (IPCC, 2006; van Delden et al., 2016). These greenspace ecosystems are widely recognized for their benefits relating to microclimate regulation, stormwater retention and biodiversity support (Connop et al., 2016; Feldman et al., 2019; Galagoda et al., 2018). Nevertheless, anthropogenic activities can strongly impact the physicochemical properties, biological communities and biogeochemical processes of these greenspace ecosystems, making them vulnerable to nutrient losses (e.g., nitrate (NO_3^-) leaching) and potential greenhouse

* Corresponding author.
E-mail address: zhishengyao@mail.iap.ac.cn (Z. Yao).

https://doi.org/10.1016/j.geoderma.2026.118113
Received 3 June 2026; Received in revised form 22 October 2026; Accepted 23 October 2026
Available online 31 October 2026
0016-7061/© 2026 The Author(s). Published by Elsevier B.V. This is an open access article under the CC BY license (http://creativecommons.org/licenses/by/4.0/).

gas (GHG) emissions (Kaye et al., 2006). Studies focusing on GHG fluxes from urban greenspaces have attracted increasing attention due to their growing role in the global biogeochemical carbon (C) and nitrogen (N) cycles. However, major questions about the magnitude, spatial controls, and seasonality of fluxes remain uncertain and highly dependent on specific regional conditions (Zhan et al., 2023).

Nitrous oxide (N_2O), carbon dioxide (CO_2) and NO_3^- leaching are important components of biogeochemical C and N cycling, potentially affecting global warming and water eutrophication (IPCC, 2021). Over a 100-year timescale, N_2O has a global warming potential 273 times greater than CO_2, and it is also the primary substance responsible for stratospheric ozone depletion (IPCC, 2021; Ravishankara et al., 2009). Urban soils are significant sources of N_2O and CO_2 emissions. Soil CO_2 emissions are closely connected to microbial turnover and the physical accessibility of organic matter to microbes and extracellular enzymes (Paustian et al., 2000). N_2O emissions, on the other hand, are connected to the reduction–oxidation processes of N in the soil, i.e., the microbial nitrification and denitrification processes (Davidson et al., 2000; Butterbach-Bahl et al., 2026). Understanding the magnitude of these emissions and the factors controlling them is essential to informing policy and guiding management efforts to mitigate climate and environmental changes. Soil water content and temperature directly impact the production and consumption of these C- and N-trace gases by affecting the metabolic activity in microorganisms and plants, as well as soil aeration and substrate availability and redistribution (Davidson and Janssens, 2006; Moyano et al., 2013; Butterbach-Bahl et al., 2013; Smith et al., 2018). For example, studies of temperate forests and grasslands have revealed significant temporal patterns in CO_2 and N_2O emissions that closely correspond with seasonal changes in soil water content and temperature. Typically, higher fluxes are associated with higher temperatures and soil water content (Yao et al., 2010; Chen et al., 2013; Luo et al., 2013). Additionally, soil NO_3^- leaching is strongly influenced by its availability and soil moisture conditions, which together determine the potential for NO_3^- transport through the soil profile (Wang et al., 2015).

Considerable work has been carried out on C and N cycling and their associated components in managed agroecosystems, as well as in natural grasslands and forests (Apostolakis et al., 2022; Li et al., 2024; Woodward et al., 2022; Yao et al., 2024; Yu et al., 2022). However, studies assessing seasonal variations in soil CO_2 and N_2O fluxes from urban greenspaces are scarce (Karim & Thomas, 2026; Künnemann et al., 2023; Livesley et al., 2010). Due to the high aesthetic and recreational standards required for greenspace landscapes, these areas are often subject to intensive maintenance including fertilization, irrigation and frequent mowing. These practices are likely to affect the availability of soil N and soil water movement, which may result in increased environmental N loss rates along gaseous and hydrologic pathways. A case study in Fort Collins, Colorado, USA demonstrated that despite occupying only 6.4% of the land area, fertilized and highly irrigated urban lawns contributed as much as 30% to regional N_2O emissions (Kaye et al., 2004). Other studies on greenspace ecosystems have reported total N_2O emissions of up to 7.6 kg N ha^{-1} yr^{-1}, comparable to or higher than those of natural grasslands, forests and managed agricultural systems (Braun & Bremer, 2018; Groffman et al., 2009; Livesley et al., 2010). Similarly, soil NO_3^- leaching rates from urban greenspace ecosystems were estimated to be 0.5–160 kg N ha^{-1} yr^{-1}, comparable to or higher than rates in natural and agricultural ecosystems (Barton & Colmer, 2006; Telenko et al., 2015; Trenholm et al., 2012; Trolove et al., 2019). However, urbanization is currently largely overlooked in IPCC reporting and projections, primarily because of limited data on C and N dynamics in urban ecosystems (IPCC, 2006, 2013).

Denmark is particularly vulnerable to the effects of climate change, such as sea-level rise and associated coastal flooding, due to its flat terrain, extensive coastline and numerous islands. To address this issue, the country plans to invest over EUR 5 billion to adapt its cities and make them more livable over the next 15–20 years (https://stateofgreen.com/en/focus-areas/water/climate-change-adaptation/). Currently, more than 70% of Denmark's population lives in urban areas, and the country provides more urban greenspaces per capita than the World Health Organization's ideal recommendation (61.7 vs. 50 m^2 per capita) (Statistics Denmark, 2025; WHO, 2010). However, the lack of data on GHG fluxes from urban greenspaces in Denmark leads to significant uncertainties in its regional and national GHG budgets. In coastal regions, there is particular interest in soil NO_3^- leaching due to widespread concerns about the eutrophication of estuarine ecosystems (Kemp et al., 2005; Paerl et al., 2006). Moreover, available data on GHG fluxes from urban soils often do not cover the non-growing season, even though a growing body of studies show that significant N_2O emissions can occur during this period (Kjær et al., 2026; Pelster et al., 2022; Wagner-Riddle et al., 2017; Wagner-Riddle et al., 2024; Wolf et al., 2010; Zhan et al., 2021). These pulses of biogeochemical cycling are often attributed to freeze–thaw effects, which increase the availability of substrates and promote the rapid growth of microbes through processes such as the dissolution, disruption of soil aggregates and the lysis of microbial cells due to osmotic shocks (Yao et al., 2010; Gao et al., 2018). Therefore, it is necessary to account for the full year dynamics of C and N associated with diverse urban greenspaces, particularly in seasonal temperate environments.

In this study, we conducted a year-round field campaign in Aarhus city, Denmark's second largest urban area. During the campaign, we measured soil N_2O and CO_2 fluxes, as well as soil NO_3^- leaching, at 40 sites within the central part of the city. These sites were representative of five common urban greenspace types: sports fields, roadside patches, residential lawns, urban parks, and urban forests. This study aimed to characterize and quantify the variation in annual N_2O and CO_2 emissions and soil NO_3^- leaching from different greenspace ecosystems, and to understand the ecosystem properties and environmental factors that control this variation. We hypothesized that soil N_2O and CO_2 fluxes as well as soil NO_3^- leaching rates would be higher in highly managed urban greenspaces, such as sports fields, due to intensive maintenance practices (e.g., fertilization), which enhance the substrate availability for microorganisms and plants (Riches et al., 2020). Additionally, we expected that fluxes during the non-growing season would contribute significantly to annual emissions, since the microbial breakdown of organic matter and the associated N cycling that occurs during freeze–thaw periods could result in significant fluxes (Wolf et al., 2010; Gao et al., 2018).

2. Materials and methods

2.1. Study area and sites

During the period from August 2024 to October 2025, we conducted an intensive field study in the central part of Aarhus city (56.140–56.181°N,10.181–10.236°E), Denmark (Fig. 1). The study region covered the inner ring road area of Aarhus City and a directly adjacent coastal urban forest area. In total, this area is about 256 ha. The study region has a temperate oceanic climate (Cfb, Köppen classification), which is characterized by warm humid summers and cold winters. In this study, we defined the period from the beginning of November to the end of March as the non-growing season (NGS) in line with the approach commonly employed in urban ecosystem studies in Nordic countries (Sieczko et al., 2023). Based on long-term meteorological data (2015–2025) (Danish Meteorological Institute, https://www.dmi.dk), the mean annual precipitation is 756 mm, and the mean annual air temperature is 9.2 °C. Mean daily air temperatures range from a minimum of −17.6 °C to a maximum of 32.3 °C, with frequent snow and frost events occurring in winter.

A greenspace map was created for the study area in Aarhus using a high-resolution 12.5 cm GeoDanmark orthophoto containing visible and near-infrared imagery (Datafordeleren, 2025). The Normalized Difference Vegetation Index (NDVI) was calculated in ArcGIS Pro, and areas with NDVI values greater than 0.1 were initially extracted as candidate

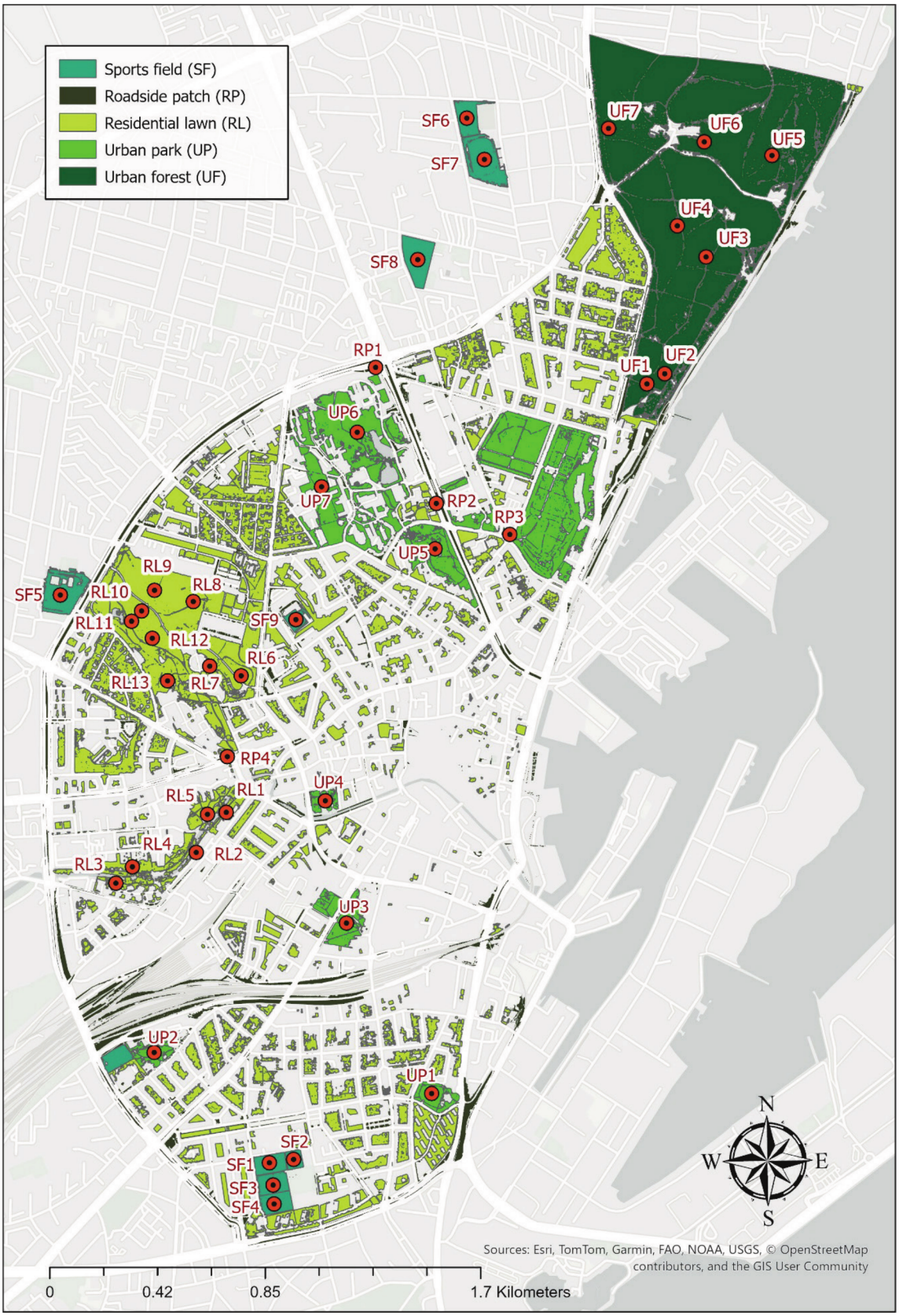


Fig. 1. Distribution of different urban greenspace types and location of the sampling sites in the Aarhus city, Denmark.

greenspace. This classification incorrectly identified some non-vegetated features, particularly shadows. Therefore, the resulting polygons were visually inspected against the original orthophoto and manually edited in ArcGIS Pro to remove the incorrectly identified areas. The final greenspace polygons were then classified into five landscape types according to their location, function and management objectives. The area of each greenspace landscape type was then calculated. The five types were as follows:

Sports fields (SF); these cover about 12.0 ha (4.7%) and are usually used for football and other field sports. They are the most common type of sports field in the region, and their management practices include routine fertilization, irrigation and mowing (Table S1). A compound fertilizer ($N:P_2O_5:K_2O = 17\%:2\%:7\%$) is applied at a rate of 80–205 kg N ha^{-1} yr^{-1} to different sites. Of these sites, only two (SF6 and SF7) were irrigated in the summer, receiving a total of about 500 mm of irrigation water per year. The grass is mowed once a week from March to April and from October to November, and twice a week from May to September. The clippings are removed from the field. The dominant grass species are *Lolium perenne* and *Poa pratensis*.

Roadside patches (RP); these cover about 24.3 ha (9.5%) and refer to road verges or nature strips. According to local management practices, the grass is occasionally mowed, and the clippings are left on the field surface. These sites do not receive fertilization or irrigation. The dominant plant species are *Lolium perenne*, *Poa pratensis*, and *Festuca rubra*.

Residential lawns (RL); these cover about 106.8 ha (41.8%) and consist primarily of lawns located near residential areas. These greenspaces are closely linked to residents' daily activities and social interactions. These sites may experience relatively high levels of human disturbance due to their frequent accessibility and use. This can result in high levels of urine and excrement from domestic animals. According to local management practices, the grass is frequently mowed in the summer, and the clippings are left on the field surface. Neither fertilization nor irrigation is applied at these sites. The dominant plant species are *Lolium perenne*, *Poa pratensis*, *Festuca rubra*, and *Trifolium repens*.

Urban parks (UP); these cover about 37.0 ha (14.5%) and are located further from residential communities than RL sites. These parks serve as critical public spaces for recreation and civic engagement. Due to lower levels of walking, resting and occasional public events, these greenspaces experience less human disturbance than RL sites. As with RL sites, the grass is frequently mowed in the summer, and the clippings are left on the field surface. These sites are not fertilized or irrigated. The dominant grass species are *Lolium perenne*, *Poa pratensis*, and *Festuca rubra*. There are also scattered trees, with the dominant species being *Acer platanoides*, *Fagus sylvatica*, *Betula pendula*, *Betula utilis*, *Quercus robur*, and *Ulmus glabra*.

Urban forest (UF); this type consists entirely of woodland areas, covering about 75.4 ha (29.5%). No fertilization or irrigation is applied to these sites. The dominant tree species are *Fagus sylvatica* (European beech), *Quercus robur*, *Larix* spp., *Acer* spp., *Fraxinus excelsior*, and *Betula* spp, while the understory vegetation is dominated by *Allium ursinum* (wild garlic).

For the sampling design, we used a stratified sampling technique (Brus & de Gruijter, 1997; Nowak et al., 2003) to determine the number of sites for each greenspace landscape type, based on the area of each type and its within-type variance of urban greenspace structure. Furthermore, we conducted a field survey of each sampling site to ensure its accessibility and representativeness. Ultimately, a total of 40 sampling sites were investigated in our study: 9 SF sites, 4 RP sites, 13 RL sites, 7 UP sites and 7 UF sites. Further information on site characteristics such as coordinates and soil physico-chemical properties are presented in Table S2.

2.2. Measurements of soil N_2O and CO_2 fluxes

Fluxes of N_2O and CO_2 were measured simultaneously using the fast closed chamber method, as described in detail by Bai et al., (2026). Briefly, one to five chamber plots (with a minimum distance of 50 m between each plot) were randomly selected at each of the sampling sites for the five greenspace landscape types. A total of 65 chamber plots were established across the five types of greenspace landscape, i.e., 18 for SF, 4 for RP, 13 for RL, 23 for UR and 7 for UF. The opaque sampling chamber was 20 cm high and 37.5 cm in diameter. For flux measurements, we carefully pushed the chamber, which had a sharpened and polished bottom edge, directly into the ground by about 1–2 cm rather than using pre-installed collars. We recognized the possibility of influencing N_2O and CO_2 fluxes due to disturbances related to chamber insertion, such as soil compression and cutting roots. For instance, Matson et al. (1990) suggest that temporarily installing a chamber may increase gas fluxes in Amazonian ecosystems. However, experiments conducted in a Costa Rican forest did not demonstrate a comparable effect of chamber installation (Keller and Reiners, 1994). The chamber had a 1 cm diameter hole in the top panel to allow pressure to equilibrate during the insertion. During gas sampling, we kept this hole closed using a pressure balance tube, as described by Hutchinson and Mosier (1981). The N_2O and CO_2 concentrations were analyzed using an Aeris MIRA Ultra N_2O/CO_2 portable gas analyzer (Aeris Technologies Inc., Hayward, CA, USA). On each sampling day, we used a chamber closure time of 5–7 min and monitored the change in headspace N_2O and CO_2 concentrations by circulating headspace air between the chamber and the analyzer at a rate of approximately 200 mL min^{-1}. To reduce the impact of midday high temperatures on N_2O and CO_2 fluxes, gas flux measurements at each site were usually conducted either in the morning (between 08:00–11:30 am) or in the afternoon (between 2:30–4:00 pm) on each sampling day. Moreover, the sampling sites were monitored in a random order on each sampling day to further minimize the potential influence of sampling. It is noteworthy that such sampling regimes may introduce a potential source of bias into the flux measurements by assuming fixed diurnal emission patterns. In this study, the minimum detection limits of gas fluxes were estimated to be 1.1 μg N $m^{-2}h^{-1}$ for N_2O and 4.1 mg C $m^{-2}h^{-1}$ for CO_2.

In general, gas flux measurements were conducted once per week throughout the entire observation period, unless interrupted by operational issues like instrument malfunction (<1% of total potential flux measurements). For the SF sites, two additional gas sampling campaigns were conducted on September 13, 2024 and April 25, 2025 to capture potentially elevated N_2O fluxes following fertilization events.

2.3. Measurements of annual soil NO_3^- leaching

To estimate the annual soil NO_3^- leaching rates, we installed Amberlite ion-exchange resins (Sigma-Aldrich, Canada) in PVC tubes (2 cm in height and 5 cm in diameter) covered with nylon mesh at the beginning of October 2024, using the method described by Sousa et al. (2016) and Wangari et al. (2024). Each tube contained 20 g of resin with an ion exchange capacity ≥ 0.6 mmol mL^{-1} was used for all greenspace landscape types. The resin bags were installed at a soil depth of 20 cm at all plots and remained in place for 12 months. After being retrieved in October 2025, the resins were extracted with a 1 M potassium chloride (KCl) solution at a resin-to-solution ratio of 1:5, and the mineral N in the extracts was analyzed colorimetrically to quantify the NO_3^- concentrations captured by the resins. Annual NO_3^- leaching rates were calculated from the measured concentrations using the following equation:

$$NO_3^- \left(kg\ N\ ha^{-1}\right) = \frac{Extract\ concentration\ \left(mg\ N\ L^{-1}\right) \times Volume\ of\ extract\ (L)}{Resin\ tube\ surface\ area\ (ha)} \times 10^{-6} \quad (1)$$

Although we used a GPS device to mark the locations of the plots where we installed the resin bags, we could not find some of them after one year. Out of the 65 plots, we only retrieved 33 samples: 6 from SF, 1 from RP, 9 from RL, 12 from UP, and 5 from UF.

2.4. Auxiliary data measurements

In addition to measuring gas fluxes and soil NO_3^- leaching rates, we collected auxiliary data, including air temperature, precipitation, snow depth, soil temperature (5 cm), soil moisture (0–5 cm), and topsoil (0–20 cm) inorganic N (NH_4^+ and NO_3^-) concentrations over the observation period. Daily precipitation and air temperature data were obtained from the Danish Meteorological Institute (https://www.dmi.dk). During each gas flux measurement, soil temperature and volumetric water content were recorded using a combined temperature and moisture HOBO sensor (Onset Computer Corporation, Bourne, MA, USA). In addition to volumetric water content, soil water content for all urban greenspace types was also reported as water-filled pore space (WFPS), which was calculated using the following the equation:

$$WFPS(\%) = \frac{Soil\ volumetric\ water\ content}{1 - \frac{Soil\ bulk\ density}{Soil\ particle\ density}} \times 100 \quad (2)$$

where the soil particle density was assumed to be 2.65 g cm^{-3}. It is important to note that using a fixed soil particle density for all five types of greenspaces may introduce uncertainties into WFPS calculations, since soil particle densities vary with soil organic matter content and soil mineralogy (Ruehlmann, 2020). Soil NH_4^+ and NO_3^- concentrations were measured at monthly intervals by collecting three replicated soil samples from each site or plot using a soil auger. After extracting the fresh soil samples with a 1 M KCl solution in a soil:solution ratio of 1:4, the NH_4^+ and NO_3^- concentrations were analyzed using a microplate spectrophotometer (Epoch 2, Agilent BioTek, USA). The details of these measurements are described in previous work (Hood-Nowotny et al., 2010). Additionally, soil NO_3^- intensity was calculated as the integrated sum of measured NO_3^- concentrations over the seasonal and annual scales (Yao et al., 2020).

2.5. Data processing and statistical analysis

The fluxes of N_2O and CO_2 were calculated based on the linear increase in gas concentration over time. This was corrected for chamber volume, sampled surface area, air temperature and atmospheric pressure (Bai et al., 2026). The N_2O and CO_2 fluxes for each site and sampling date were calculated as the mean of the fluxes from the different chamber plots. Cumulative soil N_2O and CO_2 emissions for each site were estimated by linear interpolation between sampling dates across the given period (e.g., the growing season, non-growing season and annual scale). Taking the site-level means as independent replicates for each greenspace type, an analysis of variance (ANOVA) with Turkey's range test was used to assess possible differences in cumulative N_2O and CO_2 emissions, annual NO_3^- leaching rates and environmental variables (e.g., soil temperature, WFPS and inorganic N concentrations) depending on urban greenspace type. Linear, nonlinear or multiple regression analysis was performed to explore the significant relationships between

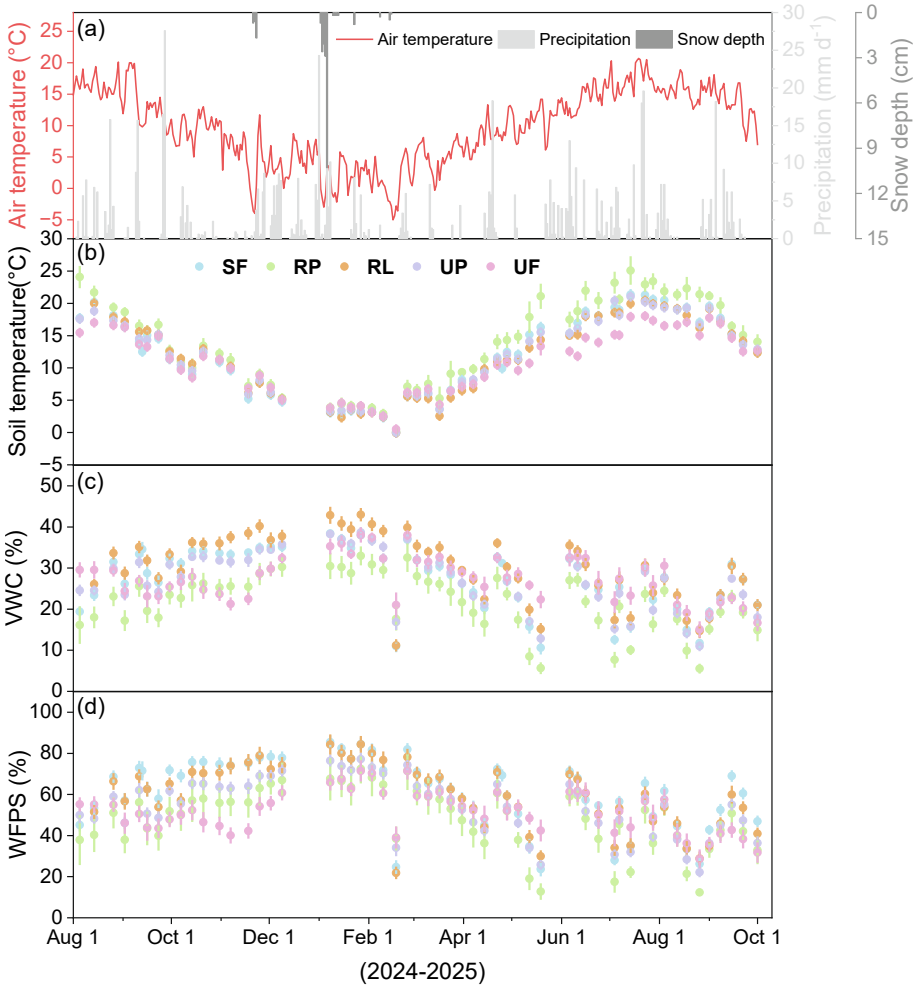


Fig. 2. Seasonal dynamics of daily precipitation, snow cover depth and air temperature (a), soil (5 cm) temperature (b), soil (0–5 cm) moisture expressed as volumetric water content (VWC) (c) or water-filled pore space (WFPS) (d) for different urban greenspace types during the study period from August 2024 to October 2025. The vertical bars in panels (b-d) indicate standard errors. The legend shown in panel (b) also applies to panels (c) and (d). SF, sports field; RP, roadside patch; RL, residential lawn; UP, urban park; UF, urban forest.

gas fluxes and environmental variables. The best regression model was selected based on the coefficient of determination (R^2). We calculated a temperature sensitivity coefficient (Q_{10}) in terms of the Arrhenius equation by plotting soil N_2O or CO_2 fluxes against soil temperature (Yao et al., 2010). All statistical analyses were performed using R software (version 4.5.2). A significant level of $P < 0.05$ was considered for all statistical tests unless stated otherwise.

3. Results

3.1. Environmental variables

During the observation period of 2024–2025, soil temperatures for all urban greenspace types exhibited a comparable seasonal pattern to that of air temperature, i.e., relatively higher temperatures occurring in the growing season compared to non-growing season (Fig. 2a, b). The annual mean soil temperatures for different greenspace types followed by the order RP (13.3 °C) > SF (11.4 °C) ≈ RL (11.1 °C) ≈ UP (11.1 °C) > UF (10.4 °C) (Table 1). Total precipitation over the year 2024–2025 was 561 mm. Snowfall and snow-covered soil were limited to a few days in the winter, with maximum snow depths reaching 10.3 cm. Soil water content for all greenspace types showed similar temporal variation, which was mainly regulated by precipitation events (and irrigation events in the case of SF). The annual mean volumetric water content was 27.6%, 22.1%, 29.5%, 26.7% and 27.5% for SF, RP, RL, UP and UF, respectively. Observed WFPS across the study period ranged between 21.9% and 85.5%, with annual means of 61.2%, 48.7%, 59.2%, 52.6% and 51.7% for SF, RP, RL, UP and UF, respectively (Fig. 2c and Table 1).

Over the entire observation period, soil NH_4^+ and NO_3^- concentrations ranged from 1.98-11.9 mg N kg^{-1} ds (dry soil) and from 0.36-5.2 mg N kg^{-1} ds, respectively, for all urban greenspace types (Fig. 3). On average, the UF site had the highest NH_4^+ concentrations with a mean value of 6.74 mg N kg^{-1} ds, while the SF had the lowest mean NH_4^+ concentration (4.38 mg N kg^{-1} ds). In contrast, the highest mean NO_3^- concentration was observed at the SF site (3.64 mg N kg^{-1} ds) and the lowest at the UF site (0.84 mg N kg^{-1} ds) (Table 1).

3.2. Soil CO_2 fluxes

During the period 2024–2025, soil CO_2 fluxes showed a similar temporal variation for all urban greenspace types, characterized by relatively higher fluxes during the growing season (Fig. 4). The CO_2 emissions varied from 30 to 620 (mean: 286) mg C $m^{-2}h^{-1}$ for SF, from 18 to 554 (mean: 220) mg C $m^{-2}h^{-1}$ for RP, from 36 to 576 (mean: 279) mg C $m^{-2}h^{-1}$ for RL, from 32 to 447 (mean: 219) mg C $m^{-2}h^{-1}$ for UP and from 36 to 432 (mean: 152) mg C $m^{-2}h^{-1}$ for UF. Linear regression analysis revealed a positive correlation between CO_2 emissions and soil temperature, as well as a negative correlation with soil volumetric water content and WFPS for all greenspace types (Table S3). However, stepwise multiple regression analysis showed that soil temperature may override the effects of soil water content and emerge as the primary factor controlling seasonal patterns of soil CO_2 fluxes. A significant exponential relationship was observed between CO_2 emissions and soil temperature for all urban greenspace types, with up to 79–90% of CO_2 variance explained by changes in soil temperature (Fig. 5 and Table S4). The estimated Q_{10} values ranged from 2.88 for UF to 3.65 for RL (Table S4).

Cumulative annual CO_2 emissions for all urban greenspace types ranged from 12.0 to 21.2 Mg C ha^{-1} yr^{-1}, of which 12.8–21.0% occurred during the non-growing season (Fig. 6 and Table 2). The cumulative annual CO_2 emissions were greatly affected by different greenspace types, with SF ≈ RL > RP ≈ UP > UF in order of emissions (Fig. 6).

Table 1
Cumulative annual nitrous oxide (N_2O) emissions as well as mean soil organic carbon (SOC), total nitrogen (TN), pH, soil temperature, volumetric water content (VWC), water-filled pore space (WFPS), concentrations of nitrate (NO_3^-), ammonium (NH_4^+) and soil NO_3^- intensity for different urban greenspace types.

Type	Annual N_2O emissions	SOC	TN	pH	Soil temperature	VWC	WFPS	NO_3^-	NH_4^+	Soil NO_3^- intensity
	(kg N ha^{-1} yr^{-1})	(mg C kg^{-1} ds)	(mg N kg^{-1} ds)	(H_2O)	(°C)	(%)	(%)	(mg N kg^{-1} ds)	(mg N kg^{-1} ds)	(g N kg^{-1} ds)
SF	4.08 ± 1.50a	25.3 ± 2.97ab	1.99 ± 0.14ab	6.97 ± 0.15ab	11.4 ± 0.33b	27.6 ± 0.74a	61.2 ± 2.33a	3.64 ± 0.24a	4.38 ± 0.37c	1.25 ± 0.08a
RP	1.25 ± 0.80ab	18.8 ± 1.69b	1.43 ± 0.19b	7.42 ± 0.12a	13.3 ± 0.93a	22.1 ± 1.49b	48.7 ± 5.26c	1.35 ± 0.28bc	4.74 ± 0.55bc	0.49 ± 0.10bc
RL	1.64 ± 0.23ab	30.1 ± 2.71a	2.33 ± 0.25a	7.14 ± 0.19a	11.1 ± 0.18b	29.5 ± 2.78a	59.2 ± 2.65ab	2.44 ± 0.38b	5.73 ± 0.32ab	0.88 ± 0.13b
UP	0.67 ± 0.12b	27.6 ± 2.59ab	2.07 ± 0.17ab	6.54 ± 0.18bc	11.1 ± 0.39b	26.7 ± 0.89ab	52.6 ± 2.33abc	2.54 ± 0.62ab	5.84 ± 0.39ab	0.91 ± 0.22ab
UF	0.88 ± 0.26b	23.4 ± 2.19ab	1.76 ± 0.17ab	6.05 ± 0.22c	10.4 ± 0.09b	27.5 ± 0.98a	51.7 ± 3.46c	0.84 ± 0.32c	6.74 ± 0.76a	0.32 ± 0.12c

Given data are means ± standard errors. SF, sports field; RP, roadside patch; RL, residential lawn; UP, urban park; UF, urban forest; ds, dry soil. The definition soil NO_3^- intensity is described in the Materials and Methods section. Different letters within the same column indicate significant differences between greenspace types at the $P < 0.05$ level.

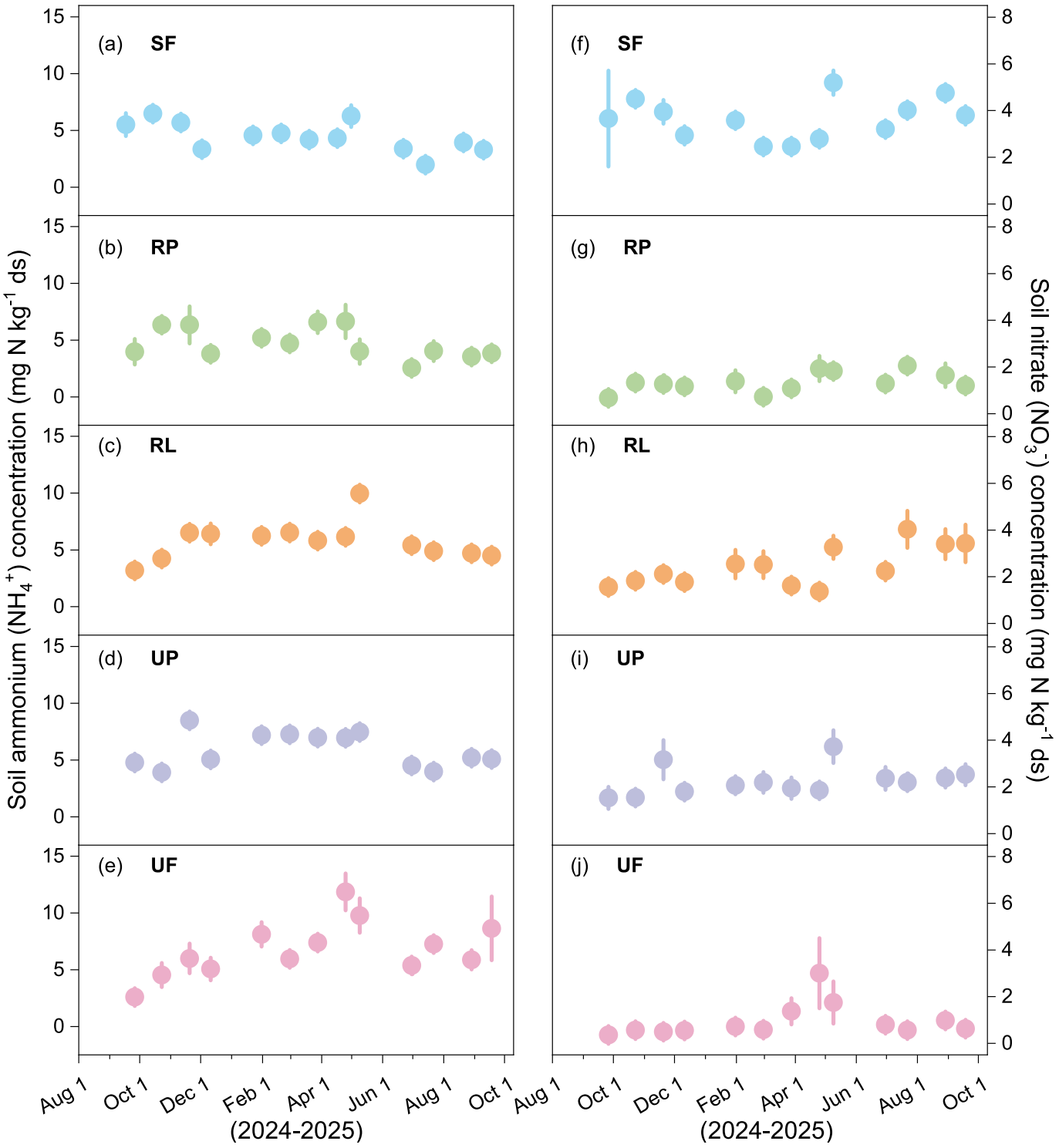


Fig. 3. Seasonal dynamics of soil ammonium (NH_4^+) (a-e) and nitrate (NO_3^-) concentrations (f-j) for different urban greenspace types during the study period from August 2024 to October 2025. The vertical bars in each panel indicate standard errors. SF, sports field; RP, roadside patch; RL, residential lawn; UP, urban park; UF, urban forest; ds, dry soil.

3.3. Soil N_2O fluxes

For the SF sites, higher N_2O emissions (27–943 μg N $m^{-2}h^{-1}$) were observed following N fertilization events during the growing season (Fig. 7). Although no N fertilization was applied at the RP, RL, and UF sites, the pronounced N_2O pulse emissions (20–206 μg N $m^{-2}h^{-1}$) also occurred episodically during the growing season. Furthermore, significant N_2O pulse emissions (33–62 μg N $m^{-2}h^{-1}$) occurred during the non-growing season at the SF and RL sites and were associated with freeze–thaw events (Fig. S1), but no such high emissions occurred at the RP and UF sites. For the UP site, soil N_2O fluxes were relatively low and stable over the entire observation period, with the magnitudes < 20 μg N $m^{-2}h^{-1}$. Across the entire observation period, linear regression analysis showed a positive correlation between N_2O fluxes and soil temperature for some greenspace types. However, the correlation between N_2O fluxes and soil volumetric water content or WFPS was insignificant

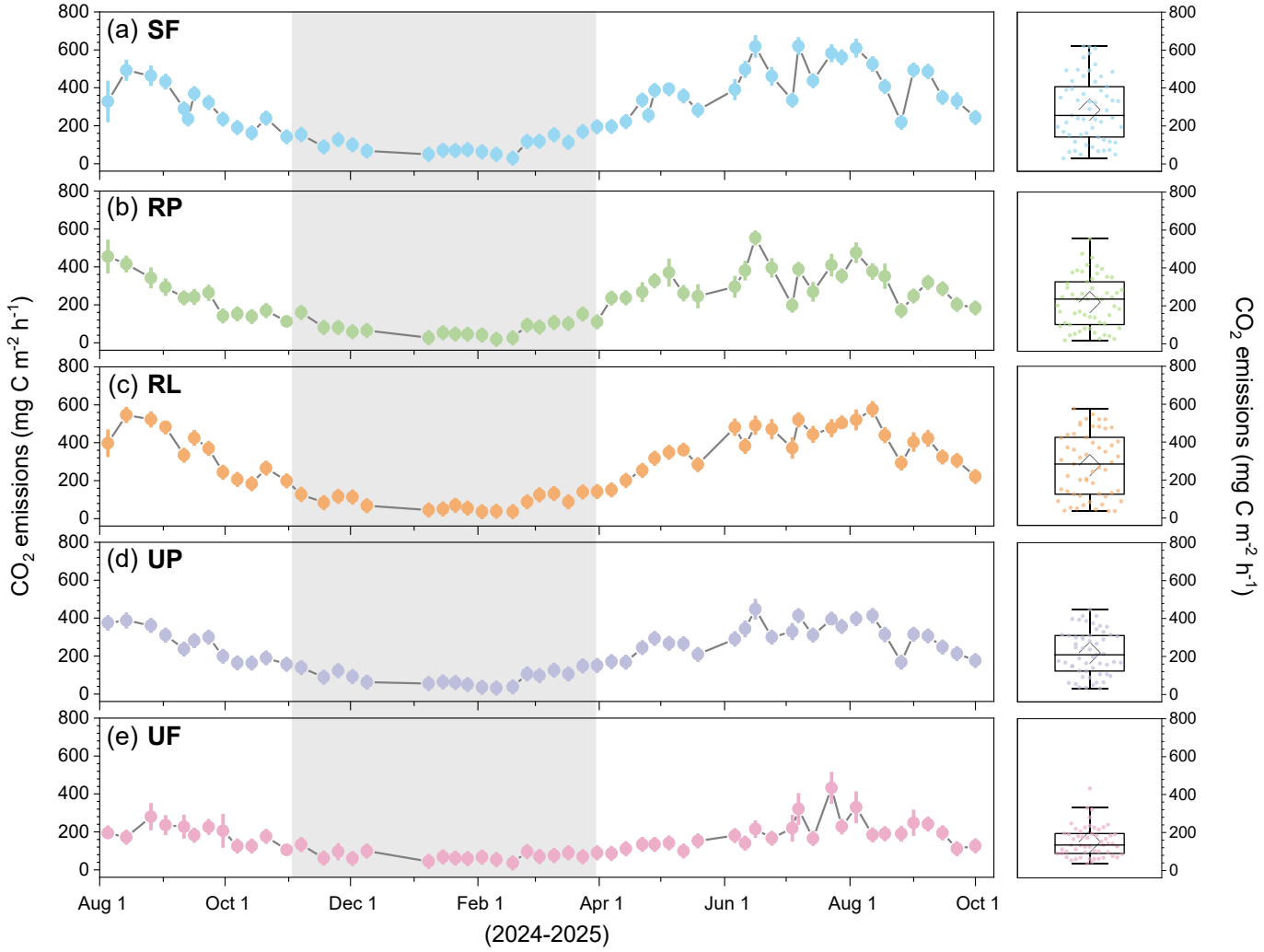


Fig. 4. Seasonal dynamics of soil carbon dioxide (CO_2) fluxes (a-e) for different urban greenspace types during the study period from August 2024 to October 2025. Grey shaded areas indicate the non-growing season. The vertical bars in each panel indicate standard errors. Boxplots on the right show the data distribution. The diamonds and solid lines inside the box represent the mean and median value, respectively. The box borders represent the 75th and 25th percentiles, and the whisker caps represent the 95th and 5th percentiles. The circle points inside each box represent the observation data. SF, sports field; RP, roadside patch; RL, residential lawn; UP, urban park; UF, urban forest.

(Table S3). We also revealed a weak but statistically significant exponential relationship between N_2O fluxes and soil temperature for the greenspace sites (i.e., RP, UF and UP) with no significant emissions during the non-growing season (Fig. 5 and Table S5). The resulting Q_{10} values for these sites ranged from 1.55 to 3.18. While the correlation with soil water content alone was not statistically significant, combining this factor with soil temperature significantly improved the estimation accuracy of N_2O variance. That is, multiple linear regression analysis showed that the temporal variation in N_2O emissions for all greenspace types was significantly regulated by the combined effects of soil temperature and WFPS across the growing season or the annual scale (Table 3).

Over the observation period, cumulative annual N_2O emissions for all urban greenspace types ranged from 0.67 to 4.08 kg N ha^{-1} yr^{-1} (Fig. 6 and Table 1). Cumulative fluxes for the growing season (from April to October) varied in the range of 0.45–3.43 kg N ha^{-1} and for the non-growing season (from November to the following March) in the range of 0.11–0.79 kg N ha^{-1}, respectively (Table 2). Depending on urban greenspace type, the contribution of the non-growing season to annual N_2O budgets was approximately 8.4–48.1%, with highest shares found for RL. Highest annual N_2O emissions were found for SF, followed by RL, RP and UF, with UP having the lowest emissions. Across all the greenspace types, the cumulative annual N_2O emissions were positively and exponentially correlated to the annual mean WFPS and soil NO_3^- intensity (Fig. 8 and Table 1), whereas they only showed a tendency with increasing soil volumetric water content (Fig. S2). Moreover, the cumulative annual N_2O emissions were positively correlated with annual CO_2 emissions (Fig. 8c).

3.4. Soil NO_3^- leaching

Over the observation period, annual NO_3^- leaching rates varied between 1.2 and 11.8 kg N ha^{-1} yr^{-1} for all urban greenspace types (Fig. 9a). Highest mean annual NO_3^- leaching rates were found for SF, while at all other urban greenspace types soil NO_3^- leaching rates were lower than 2.8 kg N ha^{-1} yr^{-1}, with no significant differences between them. Note that the annual NO_3^- leaching for RP is shown descriptively due to the insufficient number of samples obtained. Annual NO_3^- leaching rates were positively correlated with soil NO_3^- intensity, annual mean soil NO_3^- concentrations and annual mean WFPS (Fig. 9). In contrast, soil NO_3^- leaching rates tended to increase with increasing volumetric water content, but this trend was not statistically significant (Fig. S2). Across all the greenspace types, there was a positive correlation between annual NO_3^- leaching rates and cumulative annual N_2O

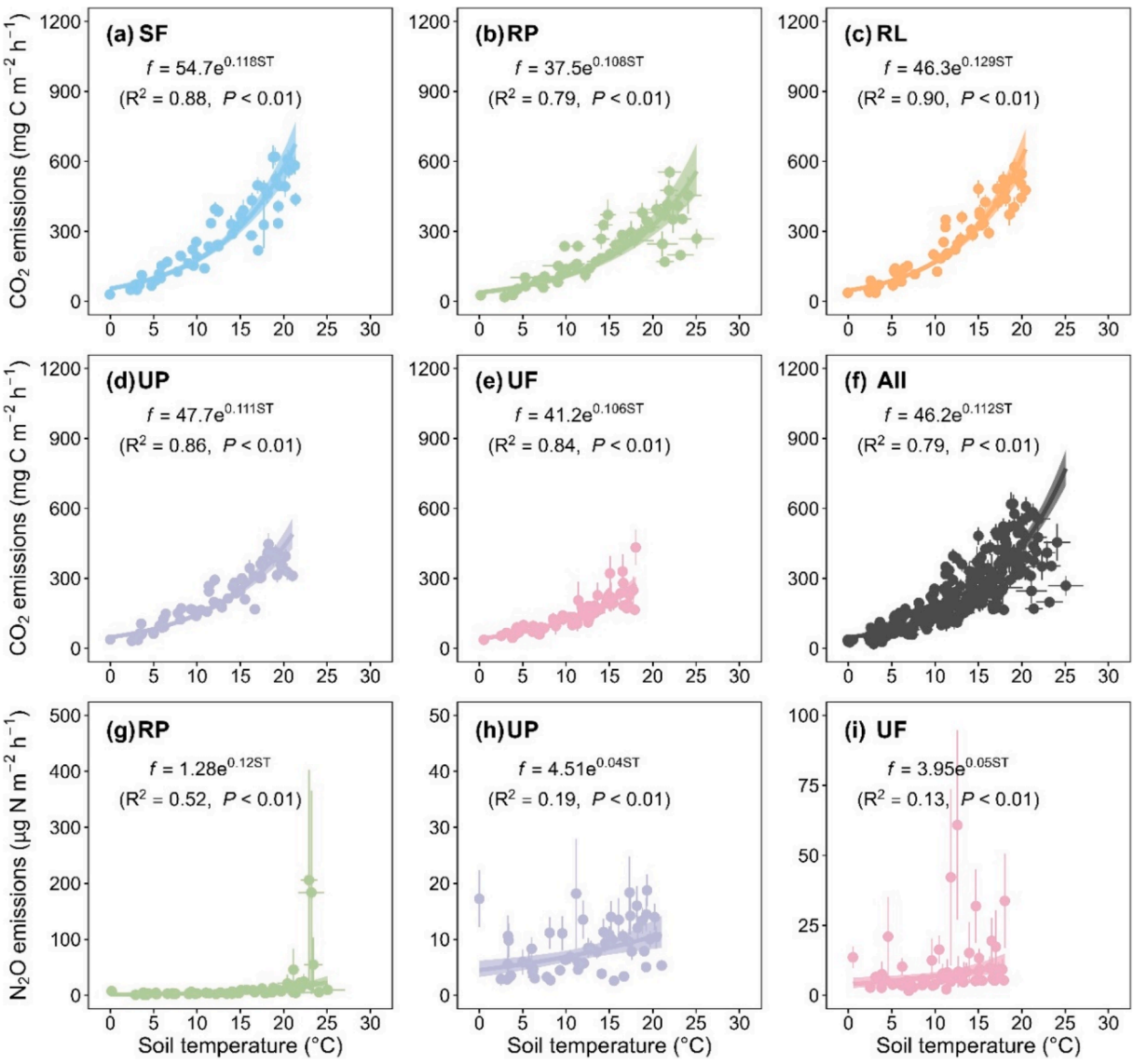


Fig. 5. Relationships between soil carbon dioxide (CO_2) fluxes and soil temperature (ST) for the individual urban greenspace types (a-e) as well as across all the greenspace types (f), and between soil nitrous oxide (N_2O) fluxes and ST for some greenspace types (g-i). The vertical and horizontal bars indicate standard errors. The shaded areas represent the 95% confidence bands. SF, sports field; RP, roadside patch; RL, residential lawn; UP, urban park; UF, urban forest.

emissions (Fig. 8d).

4. Discussion

Rapid global urbanization has substantially increased the area of urban and suburban greenspaces in Europe and other countries, altering urban biogeochemical cycles and associated C and N dynamics (Kaye et al., 2006; Trémeau et al., 2024; Zhan et al., 2023; Zhu et al., 2005). However, few studies have examined soil C- and N-trace gas fluxes from urban greenspace ecosystems in Europe (Bai et al., 2026; Clayton et al., 1997; Künnemann et al., 2023; Lu et al., 2022; Trémeau et al., 2024). Our present study offers new insights into the dynamics and magnitude of soil N_2O and CO_2 fluxes as well as soil NO_3^- leaching for different urban greenspace types in Aarhus, the second largest city in Denmark. In general, soil N_2O and CO_2 fluxes were higher during the growing season than during the non-growing season. This seasonal variation was significantly related to changes in soil temperature over time, particularly with regard to CO_2 emissions. That is, soil N_2O and CO_2 fluxes were positively correlated with soil temperature for some or all of the greenspace types (Fig. 5 and Table S4 and S5). This observation aligns with the findings of numerous studies conducted in various terrestrial ecosystems that have consistently identified soil temperature as a significant driver of the temporal dynamics of N_2O and CO_2 emissions (Chen et al., 2013; Walkiewicz et al., 2025; Wu et al., 2010; Yao et al., 2010; Butterbach-Bahl and Kiese, 2005). It is well recognized that increased soil temperature promotes microbial processes involved in N_2O and CO_2 production (Butterbach-Bahl et al., 2013; Luo et al., 2013; Smith et al., 2018). For the SF sites, higher N_2O emissions during the growing season were also the result of fertilization events that increased soil N availability for microbial nitrification and denitrification processes and associated N_2O production (Cheng et al., 2004; Li et al., 2022). Regarding soil CO_2 fluxes, higher root respiration during the growing season surely contributed significantly to the total flux, though this study did not quantify the contributions of heterotrophic and autotrophic respiration. The temperature sensitivity (Q_{10}) of N_2O and CO_2 emissions was calculated at 1.55–3.18 for N_2O and 2.88–3.65 for CO_2. Reports of Q_{10} values for N_2O fluxes in urban greenspace ecosystems are scarce. However, our estimated Q_{10} values for N_2O are comparable to or higher than those reported for natural grasslands and forests (1.79–2.11) (Phillips et al., 2014; Yu et al., 2023; Zhang et al.,

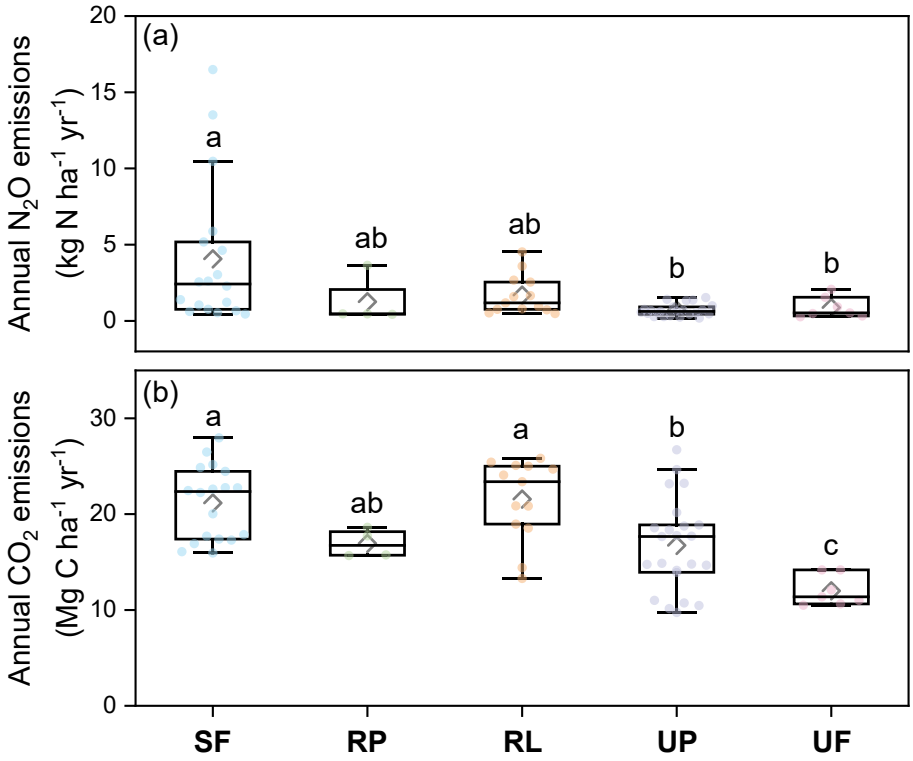


Fig. 6. Cumulative annual emissions of soil nitrous oxide (N_2O) (a) and carbon dioxide (CO_2) (b) for different urban greenspace types. In panels (a) and (b), the diamonds and solid lines inside the box represent the mean and median value, respectively. The box borders represent the 75th and 25th percentiles, and the whisker caps represent the 95th and 5th percentiles. The circle points inside each box represent the data of each plot in urban greenspace types. Different letters above the boxplots indicate significant differences among greenspace types at the $P < 0.05$ level.

Table 2
Cumulative emissions of soil nitrous oxide (N_2O) and carbon dioxide (CO_2) across the growing season (GS) and non-growing season (NGS) as well as the NGS contribution to annual budgets for different urban greenspace types.

Type	Cumulative N_2O emissions (kg N ha^{-1})			Cumulative CO_2 emissions (Mg C ha^{-1})		
	GS	NGS	NGS contribution to annual budget (%)	GS	NGS	NGS contribution to annual budget (%)
SF	3.43 ± 1.44a	0.64 ± 0.18a	15.7	18.1 ± 1.04a	3.12 ± 0.16a	14.8
RP	1.15 ± 0.80ab	0.11 ± 0.01b	8.40	14.6 ± 0.67bc	2.38 ± 0.15b	14.0
RL	0.85 ± 0.10b	0.79 ± 0.34a	48.1	18.3 ± 2.42a	2.68 ± 0.38ab	12.8
UP	0.45 ± 0.07b	0.23 ± 0.05b	33.5	12.9 ± 1.38c	2.65 ± 0.25ab	17.0
UF	0.69 ± 0.24b	0.19 ± 0.03b	22.0	9.50 ± 0.64d	2.51 ± 0.12b	21.0

Given data are means ± standard errors. SF, sports field; RP, roadside patch; RL, residential lawn; UP, urban park; UF, urban forest. Different letters within the same column indicate significant differences between greenspace types at the $P < 0.05$ level.

2020). Our estimated Q_{10} values for CO_2 fell within the range (1.76–3.76) reported for urban greenspace landscapes (Künnemann et al., 2023; Lin et al., 2025), but are relatively higher than those reported for natural ecosystems (1.51–2.1) (Bagherzadeh et al., 2008; Zhang et al., 2016). The trend of higher Q_{10} values for urban soils compared to other ecosystem types may indicate that these soils are presumably more temperature-sensitive. This suggests that climate warming may lead to disproportionately higher emissions of N_2O and CO_2 from urban greenspaces compared to other ecosystems. However, caution should be exercised when extrapolating these Q_{10} values to predict future warming responses. Since the opaque chamber suppresses photosynthesis but not respiration, the measured CO_2 flux in this study represents the total ecosystem respiration, combining autotrophic and heterotrophic components. The two processes are controlled by different factors: autotrophic respiration is primarily driven by photosynthate supply and gross primary production (GPP), with temperature being a secondary factor. In contrast, heterotrophic respiration depends on substrate quality and microbial dynamics. The seasonal coincidence of these factors with temperature can inflate an apparent Q_{10} value, which does not reflect the true intrinsic temperature sensitivity (Subke & Bahn, 2010). Moreover, as our flux measurements were only ever taken either in the morning or in the afternoon, and no correction was applied to account for the influence of diurnal temperature variations on gas fluxes, some of the flux variance may be due to the time of day rather than to seasonal or between-type differences. However, despite the fact that sites were sampled in different sequences throughout the observation period, no significant effect of daytime on soil N_2O and CO_2 fluxes was detected.

In addition to the effects of soil temperature, changes in soil water content also modified the seasonality of N_2O fluxes in this study (Table 3). Soil moisture is known to play a crucial role in N_2O flux variations by regulating the availability of electron donors (NH_4^+ and dissolved organic C (DOC)) and acceptors (NO_3^- and oxygen) to soil microbes (Butterbach-Bahl et al., 2013; Yao et al., 2010). Generally, higher WFPS can restrict oxygen diffusion in soils and promote the formation of anaerobic microsites that favor denitrification, thereby increasing N_2O production (Pan et al., 2022). Therefore, as shown in our study and others (Luo et al., 2013; Schindlbacher et al., 2004; Zhan

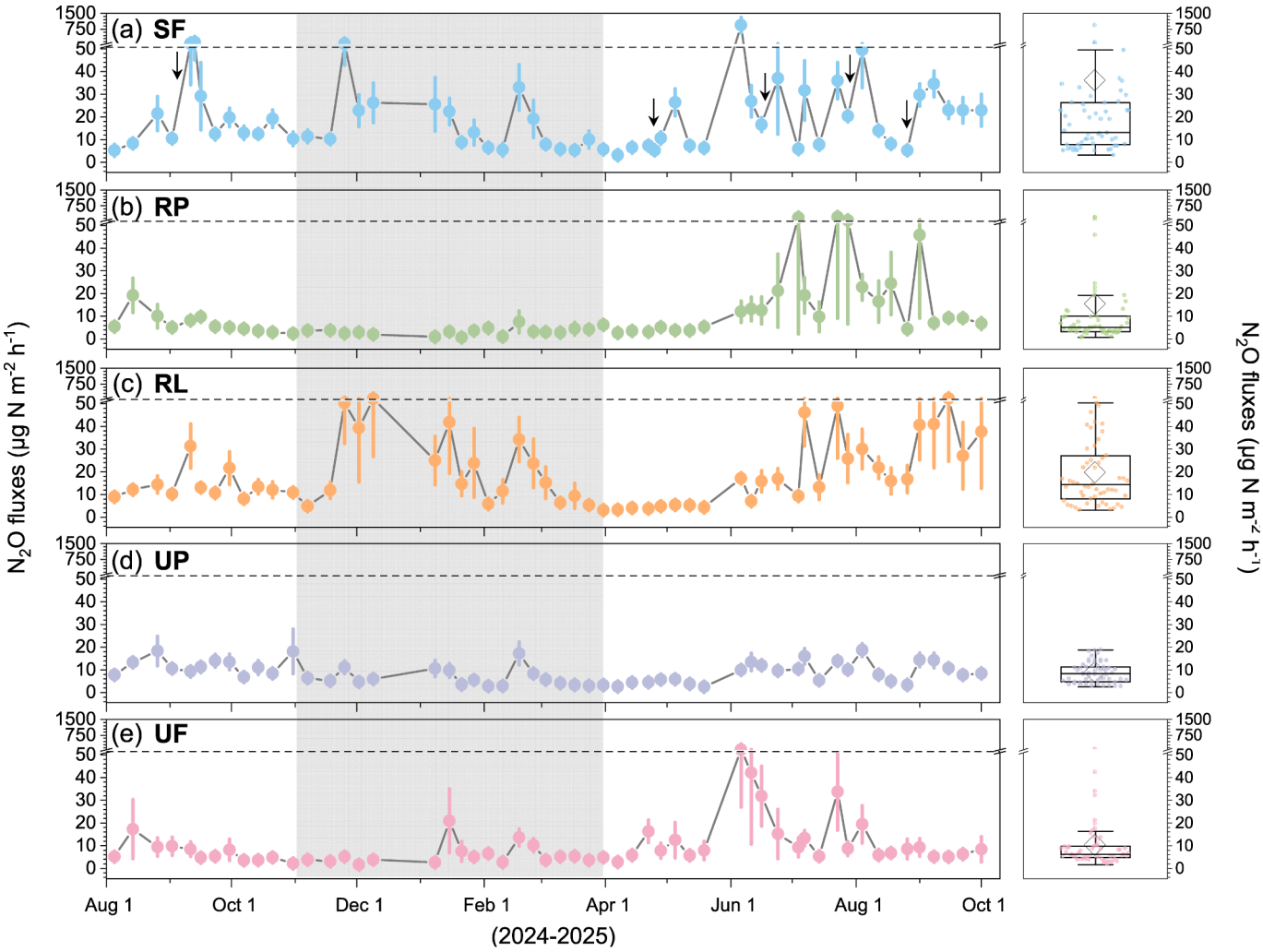


Fig. 7. Seasonal dynamics of soil nitrous oxide (N_2O) fluxes (a-e) for different urban greenspace types during the study period from August 2024 to October 2025. Grey shaded areas indicate the non-growing season. The vertical bars in each panel indicate standard errors. Boxplots on the right show the data distribution. The diamonds and solid lines inside the box represent the mean and median value, respectively. The box borders represent the 75th and 25th percentiles, and the whisker caps represent the 95th and 5th percentiles. The circle points inside each box represent the observation data. The black dotted horizontal line in each panel indicates the break point at a scale of 50 μg N $m^{-2}h^{-1}$. In panel (a), black arrows represent the time of fertilization activities. SF, sports field; RP, roadside patch; RL, residential lawn; UP, urban park; UF, urban forest.

Table 3
Results of multiple linear regression analysis regarding combined effects of soil temperature (ST, in °C) and soil volumetric water content (VWC, in %) or water filled-pore space (WFPS, in %) on soil nitrous oxide (N_2O) fluxes (f, in μg N $m^{-2}h^{-1}$) across the given period (i.e., growing season and annual scale) for different urban greenspace types.

Type	Period	Formular	R^2	P	n
RP	Annual scale	$f = 2.33ST + 0.27VWC - 23.1$	0.16	<0.05	55
UP	Annual scale	$f = 0.49ST + 0.24VWC - 3.70$	0.25	<0.01	55
UF	Annual scale	$f = 1.12ST + 1.01VWC - 29.9$	0.25	<0.01	55
SF	Growing season	$f = 4.84ST + 6.10VWC - 184$	0.06	0.31	38
RL	Growing season	$f = 2.01ST + 0.29VWC - 19.8$	0.21	<0.05	36
RP	Annual scale	$f = 2.34ST + 0.13WFPS - 23.5$	0.16	<0.05	55
UP	Annual scale	$f = 0.50ST + 0.12WFPS - 3.74$	0.25	<0.01	55
UF	Annual scale	$f = 1.11ST + 0.55WFPS - 30.6$	0.26	<0.01	55
SF	Growing season	$f = 1.48ST + 0.71WFPS - 40.1$	0.17	<0.05	38
RL	Growing season	$f = 2.01ST + 0.14WFPS - 19.5$	0.16	<0.05	36

RP, roadside patch; UP, urban park; UF, urban forest; SF, sports field; RL, residential lawn. n indicates the number of observations.

et al., 2021), the temporal variability of N_2O fluxes could be well described by the combined effects of changes in soil temperature and WFPS. Notably, while lower soil temperatures during the non-growing season could have slowed down microbial processes and associated N_2O and CO_2 emissions, higher WFPS during this period particularly for SF (mean: 72% WFPS) and RL (mean: 71% WFPS) sites may have driven the creation of local anaerobic soil environments conducive to denitrification. These two types of greenspaces (SF and RL) had relatively high SOC content (Table 1), which has a positive effect on soil available water-holding capacity (King et al., 2026). These conditions can trigger 'hot moments' of N_2O emissions during winter freeze–thaw periods (Fig. 7a, c and Fig. S1). Previous studies have also observed such pronounced N_2O emissions in conjunction with freeze–thaw events in boreal and temperate ecosystems (Gao et al., 2018; Wagner-Riddle et al., 2017; Wolf et al., 2010; Yao et al., 2025). Freeze-thaw processes can enhance N_2O emissions through mechanisms such as the release of labile substrates from microbial cell lysis, increased microbial activity during soil thawing, and temporary shifts in soil aeration conditions (de Bruijn et al., 2009; Risk et al., 2013). In this study, the non-growing season N_2O and CO_2 emissions accounted for a significant proportion of the annual budgets in all urban greenspaces, ranging from 8.4 to 48.1% (N_2O) and

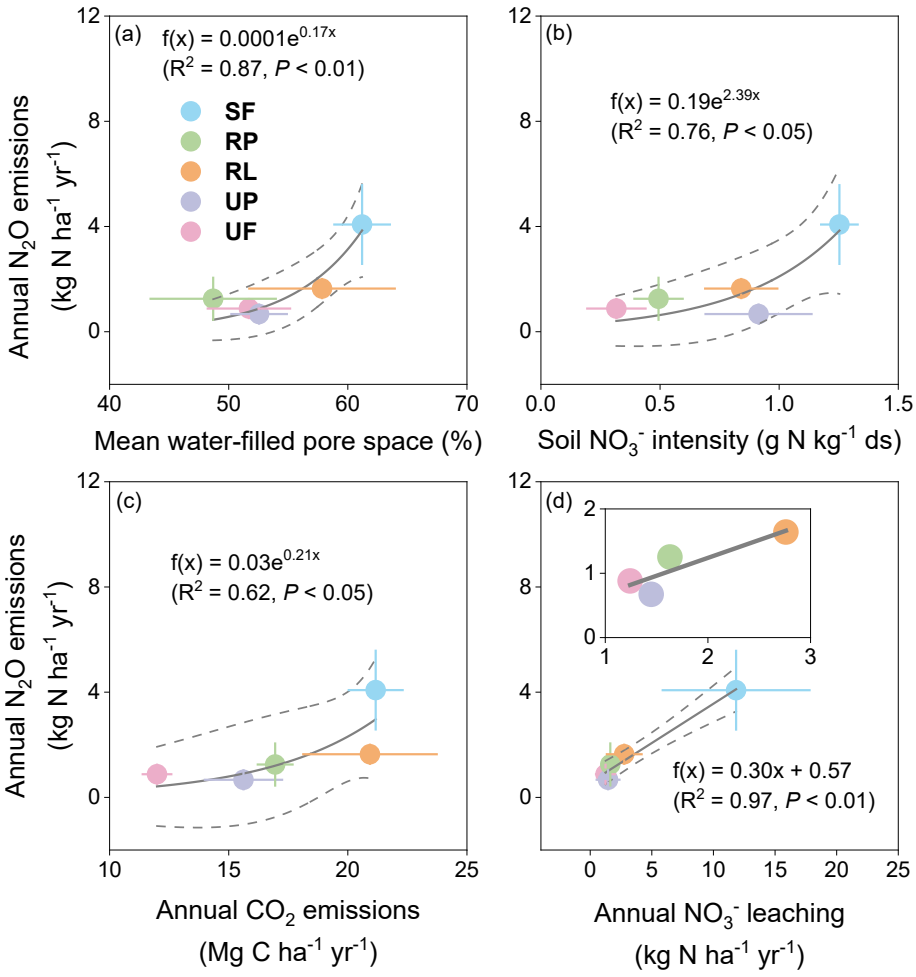


Fig. 8. Relationships between cumulative annual nitrous oxide (N_2O) emissions and annual mean water-fill pore spaces (a), soil nitrate (NO_3^-) intensity (b), cumulative annual carbon dioxide (CO_2) emissions (c), or annual nitrate (NO_3^-) leaching (d) across different urban greenspace types. The vertical and horizontal bars indicate standard errors. The dotted lines represent the 95% confidence bands. In panel (d), the inset highlights the relationship for urban greenspace types with relatively lower annual NO_3^- leaching. The legend in panel (a) also applies to panels (b-d). SF, sports field; RP, roadside patch; RL, residential lawn; UP, urban park; UF, urban forest; ds, dry soil.

12.8–21.0% (CO_2). Our results confirm the importance of the non-growing season for annual N_2O emissions, as previously reported for arable systems by Shang et al. (2024), and highlight the importance of year-round measurements in reducing uncertainties associated with GHG budgets in urban greenspace landscapes.

In our study, the cumulative annual N_2O and CO_2 emissions for all urban greenspace landscapes were 0.67–4.08 kg N ha^{-1} yr^{-1} and 12.0–21.2 Mg C ha^{-1} yr^{-1}, respectively. Our estimated N_2O emissions were within the range (0.14–4.3 kg N ha^{-1} yr^{-1}) reported for other urban greenspace ecosystems (Braun & Bremer, 2018; Davis et al., 2014; Stefaner et al., 2021; Townsend-Small et al., 2011), but were comparable to or higher than those reported for natural grasslands (0.15–0.62 kg N ha^{-1} yr^{-1}) and forests (0.04–2.53 kg N ha^{-1} yr^{-1}) (Chen et al., 2024; Czóbel et al., 2010; Guo et al., 2022; Wang et al., 2025). Our estimated CO_2 emissions also fell within the range (12.2–40.5 Mg C ha^{-1} yr^{-1}) reported for other urban greenspace ecosystems (Bezyk et al., 2023; Bogunovic et al., 2025; Künnemann et al., 2023; Livesley et al., 2010; Zhang et al., 2020), but were higher than those of natural grasslands and forests (0.44–11.3 Mg C ha^{-1} yr^{-1}, Bagherzadeh et al., 2008; Bārdule et al., 2025; Wang et al., 2026; Wang et al., 2021; Yan et al., 2021; Zhang et al., 2017). These differences between greenspaces and natural ecosystems are likely due to the direct and indirect effects of urbanization-related anthropogenic drivers on N_2O and CO_2 emissions. Direct effects include physical disturbances, burial or coverage of soil by filling material and impervious surfaces, and land management practices such as irrigation, fertilization, and frequent mowing. Indirect impacts include the urban heat island effect and the atmospheric deposition of various pollutants such as N deposition and heavy metal pollution (Pouyat et al., 2002; Xie et al., 2025).

Among the five urban greenspace landscapes, SF exhibited significantly higher cumulative annual N_2O and CO_2 emissions compared to UP and UF (Fig. 6). Intensive maintenance activities, such as fertilization and frequent irrigation are common at many SF sites. These practices are known to stimulate N_2O emissions in urban greenspaces by increasing soil N availability and the likelihood of anaerobic microsites for nitrification and/or denitrification (Gillette et al., 2016; Riches et al., 2020). This explanation was supported by the observation that cumulative annual N_2O emissions were positively correlated with soil NO_3^- intensity and soil water content across all urban greenspaces (Fig. 8 and Table 1). It should be noted that high spatial variability in N_2O fluxes was observed at the SF sites over the measurement period due to management heterogeneity. Due to topdressing, which involves applying a layer of compost to the soil surface, these sites were identified as emission hotspots, with cumulative annual N_2O emissions ranging from 5.53 to 13.5 kg N ha^{-1} yr^{-1} (Table S2). Across all SF sites, cumulative annual N_2O emissions tended to increase with higher N application rates (Fig. S3). Moreover, frequent maintenance activities at SF sites enhance plant productivity and root biomass, thereby increasing soil autotrophic

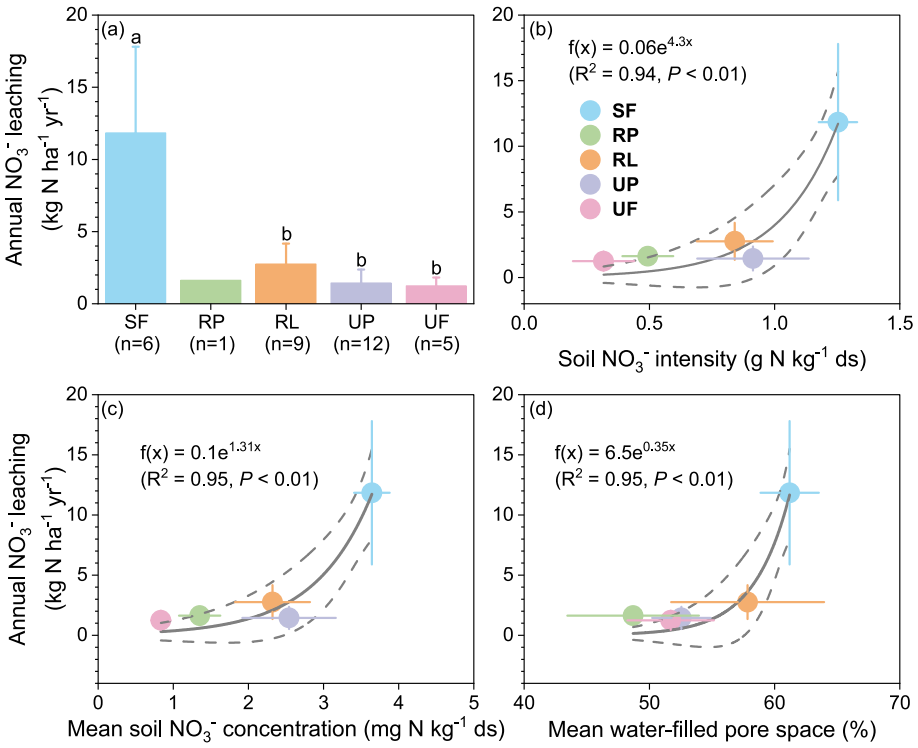


Fig. 9. Annual nitrate (NO_3^-) leaching for different urban greenspace types (a), and the relationships between annual NO_3^- leaching and soil nitrate (NO_3^-) intensity (b), annual mean soil NO_3^- concentrations (c), or annual mean water-filled pore space (d) across different urban greenspace types. The data in brackets of panel (a) indicate the number of observations in each greenspace type. Due to the insufficient number of observations, the annual NO_3^- leaching for roadside patch (RP) is shown descriptively. The vertical and/or horizontal bars indicated standard errors. Different letters above the columns indicate significant differences among greenspace types at the $P < 0.05$ level. SF, sports field; RP, roadside patch; RL, residential lawn; UP, urban park; UF, urban forest; ds, dry soil. The dotted lines represent the 95% confidence bands. Both panels share the same y-axis representing annual NO_3^- leaching.

and heterotrophic respiration (Thompson & Kao-Kniffin, 2019). The positive relationship between cumulative annual N_2O and CO_2 emissions also suggests a strong coupling between C and N cycling processes in urban greenspace ecosystems. This relationship was previously observed by Xu et al. (2008) in other terrestrial ecosystems. Higher soil CO_2 emissions likely reflect enhanced microbial respiration and organic matter decomposition, which may stimulate nitrification and denitrification processes responsible for N_2O production (Xu et al., 2008). Additionally, despite having similar management practices, RL had relatively higher soil N_2O and CO_2 fluxes than UP. This difference was likely linked to the varying frequency and intensity of human disturbances at the two sites. RL was subject to higher levels of input from domestic animal urine and excrement, which are direct sources of labile C and N for microbial processes, thereby increasing soil N_2O and CO_2 emissions (Braun et al., 2023). Compared to other greenspace types (e.g., SF, RP and RL), UF showed relatively lower N_2O and CO_2 emissions. This is likely linked to compounding factors specific to UF. Specifically, the microclimatic shading effect of the tree canopy would keep soil temperatures lower than in other open lawn systems, thereby reducing microbial activity and associated N_2O and CO_2 production (Künnemann et al., 2023). Moreover, litter inputs at UF are dominated by more recalcitrant woody or leaf litter (e.g., beech and oak) rather than the fast-cycling, easily decomposable grass biomass and clippings characteristic of lawn systems. This may also lower biogeochemical cycling and associated N_2O and CO_2 emissions. Notably, our study includes the RP, a greenspace type that is comparatively rarely studied. The RP sites had the highest annual mean soil temperature of the five types. This is likely due to a localized urban heat effect, as adjacent impervious road and pavement surfaces can absorb and store solar radiation, thereby increasing soil temperatures at RP (Pouyat et al., 2002; Cheela et al., 2021). However, despite having the highest annual mean soil temperature, the RP did not exhibit the highest N_2O and CO_2 emissions. This pattern is consistent with a moisture limitation effect, since the RP had the lowest annual mean WFPS among all types. While higher soil temperatures could stimulate microbial activity, the effect of temperature was offset by concurrent soil drying, limiting microbial C and N transformations and associated N_2O and CO_2 emissions (Huang et al., 2025). Given the limited data on RP in this study, future research is needed that integrates multiple sites and years of monitoring with process-oriented or spatially distributed hydrological-biogeochemical models. This will allow for a more rigorous quantification of the hydrothermal effects on N_2O and CO_2 emissions from urban greenspace ecosystems.

At the city level, the average annual N_2O and CO_2 emissions, weighed by the areal extent of the different urban greenspace types, were estimated at 1.35 kg N ha^{-1} yr^{-1} and 17.2 Mg C ha^{-1} yr^{-1}, respectively. Given that reliable estimates of the total land area covered by urban greenspace landscapes in Denmark and worldwide are not available, the upscaling exercise was restricted to Aarhus. Multiplying the total area of urban greenspaces in Aarhus (256 ha) by our observed area-weighted annual N_2O and CO_2 emissions yields total N_2O and CO_2 emissions of 346 kg N yr^{-1} and 4403 Mg C yr^{-1}, respectively. Considering that N_2O and CO_2 emissions from fuel combustion and industrial processes may decline in the future due to various control measures (Nielsen et al., 2023) and that greenspace areas are expected to increase to meet the demands of rapid global urbanization, the importance of urban greenspace emissions to national GHG inventory may significantly increase in future.

Annual NO_3^- leaching rates for all urban greenspace landscapes ranged from 1.2 to 11.8 kg N ha^{-1} yr^{-1} (Fig. 9). These rates were within the range reported for other urban greenspace ecosystems in USA (0.5–25.2 kg N ha^{-1} yr^{-1}, Groffman et al., 2009) and for natural forests (1–40 kg N ha^{-1} yr^{-1}, Borken & Matzner, 2004; MacDonald et al., 2002; Wangari et al., 2024). Of the five urban greenspace types, SF exhibited the highest annual NO_3^- leaching rates. We also found a strong positive

relationship between annual NO_3^- leaching and N_2O emissions across all urban greenspaces. This indicates that intensive practices like fertilization at SF sites can result in significant N losses, including gaseous fluxes and hydrologic losses (Cameron et al., 2013). Similar relationships between N_2O emissions and NO_3^- leaching have been reported in other managed ecosystems, where increased N inputs stimulate both loss pathways (Maharjan et al., 2014; Qasim et al., 2021). However, Zhou et al. (2013) reported significant trade-offs between NO_3^- leaching and N_2O emissions under certain N management practices. Moreover, our study corroborates the findings of other studies showing that soil NO_3^- leaching is often controlled by soil water volume and topsoil NO_3^-concentrations (Fu et al., 2017). Higher soil water and NO_3^- availability resulted in soil NO_3^- leaching rates being higher at SF than at other greenspaces (Fig. 9). At the city scale, the area-weighted annual NO_3^- leaching rates for urban greenspaces were calculated at 2.44 kg N ha^{-1} yr^{-1}. Using the same scaling-up approach applied to soil N_2O and CO_2 emissions, we estimated the total annual soil NO_3^- leaching from Aarhus urban greenspaces to be approximately 625 kg N yr^{-1}. Although this figure is considerably lower than the total annual NO_3^- leaching from Danish agricultural systems (160 Gg N yr^{-1}) (Danish Environmental Protection Agency, 2009), it can still induce 'off-site' indirect N_2O emissions. Further research is necessary to investigate the dynamics of soil NO_3^- leaching from urban greenspace landscapes using a long-established, classical method like lysimeters in order to address the key limitations of the resin-based method (Wyland & Jackson, 1993).

5. Conclusions

This work presents the first year-round dataset of soil N_2O and CO_2 fluxes as well as soil NO_3^- leaching for various urban greenspace types in Denmark. Our study suggests that the temporal variability of soil N_2O fluxes is regulated by the synergistic changes in soil water content and temperature, though neither factor exhibited a strong individual effect. The variance of soil CO_2 fluxes is triggered by changes in soil water content and temperature, but the effect of soil temperature overrides that of soil water content. As expected, the non-growing season makes an indispensable contribution to annual N_2O and CO_2 emissions, highlighting the importance of year-round measurements to accurately estimate annual C- and N-trace gas budgets. Among the five greenspace landscape types, sports fields exhibited the highest annual losses of soil N_2O and NO_3^- leaching, while significantly lower values were observed in urban parks and forests. The differences in soil N losses among greenspace types are likely driven by variations in soil water content and soil NO_3^- availability. Annual CO_2 emissions across all urban greenspace types showed a similar pattern to N_2O, with both exhibiting a positive correlation. At the city level, the average annual N_2O and CO_2 emissions and soil NO_3^- leaching, weighted by the areal extent of the different urban greenspace types, were estimated at 1.35 kg N ha^{-1} yr^{-1} (N_2O), 17.2 Mg C ha^{-1} yr^{-1} (CO_2) and 2.44 kg N ha^{-1} yr^{-1} (NO_3^- leaching), respectively. Considering the relatively high soil N losses particularly N_2O emissions, from urban greenspace ecosystems and the increasing area of these ecosystems due to rapid global urbanization, further studies are required to quantify the contribution of greenspace GHG emissions at the regional or national level and to investigate mitigation efforts.

CRediT authorship contribution statement

Xiao Bai: Writing – original draft, Investigation, Formal analysis, Data curation. **Tom Cripps:** Visualization. **Arezoo Taghizadeh-Toosi:** Writing – review & editing, Resources, Investigation. **Shuoyue Wang:** Visualization. **Klaus Butterbach-Bahl:** Writing – review & editing, Supervision, Resources, Funding acquisition, Conceptualization. **Zhisheng Yao:** Writing – review & editing, Writing – original draft, Supervision, Methodology, Investigation, Formal analysis.

Declaration of competing interest

The authors declare that they have no known competing financial interests or personal relationships that could have appeared to influence the work reported in this paper.

Acknowledgments

This research has been supported by "Pioneer Center for Research in Sustainable Agricultural Futures" (Land-CRAFT), DNRF grant number P2, Aarhus University, Denmark. Further funding for ZY was provided by the Beijing Natural Science Foundation (8242042). We would like to acknowledge Aarhus Kommune for granting access to the sports fields and for providing information on management activities. We thank our technicians Lars Norge Andreassen and Joakim Voltelen Klausen for their assistance with measurements and equipment operation. We also thank Favour Modupe Ayedun and Elena Petersen for laboratory assistance, Johanne Jensen for assistance with fieldwork, Noa Emily Millman for support with ArcGIS Pro, and Elizabeth Gachibu Wangari for technical guidance and analytical support. XB acknowledges support from the China Scholarship Council.

Appendix A. Supplementary data

Supplementary data to this article can be found online at https://doi.org/10.1016/j.geoderma.2026.118113.

Data availability

Data will be made available on request.

References

Danish Environmental Protection Agency. (2009). Status and trends of aquatic environment and agricultural practice: Danish monitoring and action programmes in accordance with the Nitrates Directive (1991/676/EEC). Ministry of the Environment.

Apostolakis, A., Schöning, I., Klaus, V.H., Michalzik, B., Bischoff, W.-A., Boeddinghaus, R.S., Bolliger, R., Fischer, M., Hölzel, N., Kandeler, E., Kleinebecker, T., Manning, P., Marhan, S., Neyret, M., Oelmann, Y., Prati, D., van Kleunen, M., Schwarz, A., Schurig, E., Schrumpf, M., 2022. Direct and plant community mediated effects of management intensity on annual nutrient leaching risk in temperate grasslands. Nutr. Cycl. Agroecosyst. 123 (3), 83–104. https://doi.org/10.1007/s10705-022-10209-1.

Bagherzadeh, A., Brumme, R., Beese, F., 2008. Temperature dependence of carbon mineralization and nitrous oxide emission in a temperate forest ecosystem. J. For. Res. 19 (2), 107–112. https://doi.org/10.1007/s11676-008-0018-3.

Bai, X., Cripps, T., Serra, J., Butterbach-Bahl, K., Yao, Z., 2026. Spatial and temporal variability of CO_2, N_2O and CH_4 fluxes from an urban park in Denmark. Biogeosciences 23 (9), 3207–3223. https://doi.org/10.5194/bg-23-3207-2026.

Bārdule, A., Laiho, R., Jauhiainen, J., Soosaar, K., Lazdiņš, A., Armolaitis, K., Butlers, A., Čiuldienė, D., Haberl, A., Kull, A., 2025. Annual net CO_2 fluxes from drained organic soils used for agriculture in the hemiboreal region of Europe. Biogeosciences 22 (16), 4241–4259. https://doi.org/10.5194/bg-22-4241-2025.

Barton, L., Colmer, T.D., 2006. Irrigation and fertiliser strategies for minimising nitrogen leaching from turfgrass. Agric Water Manag 80 (1), 160–175. https://doi.org/10.1016/j.agwat.2005.07.011.

Bezyk, Y., Dorodnikov, M., Górka, M., Sówka, I., Sawiński, T., 2023. Temperature and soil moisture control CO_2 flux and CH_4 oxidation in urban ecosystems. Geochemistry 83 (3), 125989. https://doi.org/10.1016/j.chemer.2023.125989.

Bogunovic, I., Galic, M., Percin, A., Geng, S., Pereira, P., 2025. The Role of Grassland Land Use in Enhancing Soil Resilience and climate Adaptation in Periurban Landscapes. Agronomy 15 (7). https://doi.org/10.3390/agronomy15071589.

Borken, W., Matzner, E., 2004. Nitrate leaching in forest soils: an analysis of long-term monitoring sites in Germany. J. Plant Nutr. Soil Sci. 167 (3), 277–283. https://doi.org/10.1002/jpln.200421354.

Braun, R.C., Bremer, D.J., 2018. Nitrous oxide emissions from turfgrass receiving different irrigation amounts and nitrogen fertilizer forms. Crop Sci. 58 (4), 1762–1775. https://doi.org/10.2135/cropsci2017.11.0688.

Braun, R.C., Straw, C.M., Soldat, D.J., Bekken, M.A.H., Patton, A.J., Lonsdorf, E.V., Horgan, B.P., 2023. Strategies for reducing inputs and emissions in turfgrass systems. Crop Forage Turfgrass Manage. 9 (1). https://doi.org/10.1002/cft2.20218.

Brus, D.J., de Gruijter, J.J., 1997. Random sampling or geostatistical modelling? Choosing between design-based and model-based sampling strategies for soil (with discussion). Geoderma 80 (1), 1–44. https://doi.org/10.1016/S0016-7061(97)00072-4.

Butterbach-Bahl, K., Baggs, E.M., Dannenmann, M., Kiese, R., Zechmeister-Boltenstern, S., 2013. Nitrous oxide emissions from soils: how well do we understand the processes and their controls? Philos. Trans. R. Soc. Lond. B Biol. Sci. 368 (1621), 20130122. https://doi.org/10.1098/rstb.2013.0122.

Butterbach-Bahl, K., Philippot, L., Serra, J., Silver, W.L., Ogle, S., Abalos, D., 2026. Three decades of soil N_2O research insights and gaps. Glob. Chang. Biol. 32, e71308. https://doi.org/10.1111/gcb.71038.

Butterbach-Bahl, Klaus, Kiese, Ralf, 2005. Significance of Forests as Sources for N_2O and NO. NATO Science Series IV: Earth and Environmental Sciences. Springer Netherlands, Dordrecht, ISBN 9781402034459, pp. 173–191. https://doi.org/10.1007/1-4020-3447-4_10. http://link.springer.com/10.1007/1-4020-3447-4_10.

Cameron, K.C., Di, H.J., Moir, J.L., 2013. Nitrogen losses from the soil/plant system: a review. Ann. Appl. Biol. 162 (2), 145–173. https://doi.org/10.1111/aab.12014.

Cheela, V.S., John, M., Biswas, W., Sarker, P., 2021. Combating urban heat island effect—A review of reflective pavements and tree shading strategies. Buildings 11 (3), 93. https://doi.org/10.3390/buildings11030093.

Chen, W., Jia, X., Zha, T., Wu, B., Zhang, Y., Li, C., Wang, X., He, G., Yu, H., Chen, G., 2013. Soil respiration in a mixed urban forest in China in relation to soil temperature and water content. Eur. J. Soil Biol. 54, 63–68. https://doi.org/10.1016/j.ejsobi.2012.10.001.

Chen, Y., Han, M., Qin, W., Hou, Y., Zhang, Z., Zhu, B., 2024. Effects of whole-soil warming on CH_4 and N_2O fluxes in an alpine grassland. Glob. Chang. Biol. 30 (1), e17033. https://doi.org/10.1111/gcb.17033.

Cheng, W., Tsuruta, H., Chen, G., Yagi, K., 2004. N_2O and NO production in various Chinese agricultural soils by nitrification. Soil Biol. Biochem. 36 (6), 953–963. https://doi.org/10.1016/j.soilbio.2004.02.012.

Clayton, H., McTaggart, I.P., Parker, J., Swan, L., Smith, K.A., 1997. Nitrous oxide emissions from fertilised grassland: a 2-year study of the effects of N fertiliser form and environmental conditions. Biol. Fertil. Soils 25 (3), 252–260. https://doi.org/10.1007/s003740050311.

Connop, S., Vandergert, P., Eisenberg, B., Collier, M.J., Nash, C., Clough, J., Newport, D., 2016. Renaturing cities using a regionally-focused biodiversity-led multifunctional benefits approach to urban green infrastructure. Environ. Sci. Policy 62, 99–111. https://doi.org/10.1016/j.envsci.2016.01.013.

Czóbel, S., Horváth, L., Szirmai, O., Balogh, J., Pintér, K., Németh, Z., ÜRmös, Z., Grosz, B., & Tuba, Z. (2010). Comparison of N_2 O and CH_4 fluxes from Pannonian natural ecosystems. *European Journal of Soil Science*, *61*(5), 671–682. https://doi.org/10.1111/j.1365-2389.2010.01275.x.

Datafordeleren, 2025. GeoDanmark Ortofoto Fildownload (Raster). https://datafordeler.dk/dataoversigt/geodanmark-ortofoto/geodanmark-ortofoto-fildownload-raster/ (Accessed: August 2025).

Davidson, E.A., Keller, M., Erickson, H.E., Verchot, L.V., Veldkamp, E., 2000. Testing a conceptual model of soil emissions of nitrous and nitric oxides. Bioscience 50 (8), 667–680. https://doi.org/10.1641/0006-3568(2000)050[0667:TACMOS]2.0.CO;2.

Davidson, Eric A., Janssens, Ivan A., 2006. Temperature sensitivity of soil carbon decomposition and feedbacks to climate change. Nature 440 (7081), 165–173. https://doi.org/10.1038/nature04514. https://www.nature.com/articles/nature04514.

Davis, M.P., David, M.B., Voigt;, T.B., Mitchell, C.A., 2014. Effect of nitrogen addition on Miscanthus × giganteus yield, nitrogen losses, and soil organic matter across five sites. GCB Bioenergy 7 (6), 1222–1231. https://doi.org/10.1111/gcbb.12217.

de Bruijn, A.M.G., Butterbach-Bahl, K., Blagodatsky, S., Grote, R., 2009. Model evaluation of different mechanisms driving freeze–thaw N_2O emissions. Agr Ecosyst Environ 133 (3), 196–207. https://doi.org/10.1016/j.agee.2009.04.023.

Feldman, A., Foti, R., Montalto, F., 2019. Green Infrastructure Implementation in Urban Parks for Stormwater Management. Journal of Sustainable Water in the Built Environment 5 (3), 05019003. https://doi.org/10.1061/JSWBAY.0000880.

Fu, J., Gasche, R., Wang, N., Lu, H., Butterbach-Bahl, K., Kiese, R., 2017. Impacts of climate and management on water balance and nitrogen leaching from montane grassland soils of S-Germany. Environ. Pollut. 229, 119–131. https://doi.org/10.1016/j.envpol.2017.05.071.

Galagoda, R.U., Jayasinghe, G.Y., Halwatura, R.U., Rupasinghe, H.T., 2018. The impact of urban green infrastructure as a sustainable approach towards tropical micro-climatic changes and human thermal comfort. Urban For. Urban Green. 34, 1–9. https://doi.org/10.1016/j.ufug.2018.05.008.

Gao, D., Zhang, L., Liu, J., Peng, B., Fan, Z., Dai, W., Jiang, P., Bai, E., 2018. Responses of terrestrial nitrogen pools and dynamics to different patterns of freeze-thaw cycle: a meta-analysis. Glob. Chang. Biol. 24 (6), 2377–2389. https://doi.org/10.1111/gcb.14010.

Gillette, K.L., Qian, Y., Follett, R.F., Del Grosso, S., 2016. Nitrous oxide emissions from a golf course fairway and rough after application of different nitrogen fertilizers. J. Environ. Qual. 45 (5), 1788–1795.

Groffman, P.M., Williams, C.O., Pouyat, R.V., Band, L.E., Yesilonis, I.D., 2009. Nitrate Leaching and Nitrous Oxide Flux in Urban Forests and Grasslands. J. Environ. Qual. 38 (5), 1848–1860. https://doi.org/10.2134/jeq2008.0521.

Guo, Y., Dong, Y., Peng, Q., Li, Z., He, Y., Yan, Z., Qin, S., 2022. Effects of nitrogen and water addition on N_2O emissions in temperate grasslands, northern China. Appl. Soil Ecol. 177, 104548. https://doi.org/10.1016/j.apsoil.2022.104548.

Hood-Nowotny, R., Umana, N.-H.-N., Inselbacher, E., Oswald-Lachouani, P., Wanek, W., 2010. Alternative Methods for Measuring Inorganic, Organic, and Total Dissolved Nitrogen in Soil. Soil Sci. Soc. Am. J. 74 (3), 1018–1027. https://doi.org/10.2136/sssaj2009.0389.

Huang, K., Wu, D., Liu, D., Duan, Y., Dörsch, P., Butterbach-Bahl, K., Fang, X., Liu, Y., Wang, C., Yu, H., Qu, L., Xu, J., Gurmesa, G.A., Kang, R., Peng, S., Hobbie, E.A., Ju, X., Hu, S., Phillips, O.L., Gundersen, P., Zhu, W., Homyak, P.M., Fang, Y., 2025. Climate warming reduces soil gaseous nitrogen losses in a temperate forest. PNAS 122 (48), e2513401122. https://doi.org/10.1073/pnas.2513401122.

Hutchinson, G.L., Mosier, A.R., 1981. Improved soil cover method for field measurement of nitrous oxide fluxes. Soil Sci. Soc. Am. J. 45 (2), 311–316. https://doi.org/10.2136/sssaj1981.03615995004500020017x.

IPCC, 2006. 2006 *IPCC Guidelines for National Greenhouse Gas Inventories*. H. S. Eggleston, L. Buendia, K. Miwa, T. Ngara, & K. Tanabe (Eds.). Institute for Global Environmental Strategies (IGES), Hayama, Japan.

IPCC, 2013. Climate Change 2013: The Physical Science Basis. Contribution of Working Group I to the Fifth Assessment Report of the Intergovernmental Panel on Climate Change. Stocker, T.F., et al. (Eds.). Cambridge University Press, Cambridge, United Kingdom and New York, NY, USA. https://doi.org/10.1017/CBO9781107415324.

IPCC, 2021. Climate Change 2021: The Physical Science Basis. Contribution of Working Group I to the Sixth Assessment Report of the Intergovernmental Panel on Climate Change. Masson-Delmotte, V., Zhai, P., Pirani, A., Connors, S.L., Péan, C., Berger, S., Caud, N., Chen, Y., Goldfarb, L., Gomis, M.I., Huang, M., Leitzell, K., Lonnoy, E., Matthews, J.B.R., Maycock, T.K., Waterfield, T., Yelekçi, O., Yu, R., Zhou, B. (Eds.). Cambridge University Press, Cambridge, United Kingdom and New York, NY, USA. https://doi.org/10.1017/9781009157896.

Karim, M.R., Thomas, S.C., 2026. Urban tree Channeling of Soil methane and Nitrous Oxide and its Mitigation using Biochar. Environ. Sci. Technol. 60 (18), 13437–13451. https://doi.org/10.1021/acs.est.6c01265.

Kaye, J., Groffman, P., Grimm, N., Baker, L., Pouyat, R., 2006. A distinct urban biogeochemistry? Trends Ecol. Evol. 21 (4), 192–199. https://doi.org/10.1016/j.tree.2005.12.006.

Kaye, J.P., Burke, I.C., Mosier, A.R., Pablo Guerschman, J., 2004. Methane and nitrous oxide fluxes from urban soils to the atmosphere. Ecol. Appl. 14 (4), 975–981. https://doi.org/10.1890/03-5115.

Keller, M., Reiners, W.A., 1994. Soil-atmosphere exchange of nitrous oxide, nitric oxide, and methane under secondary succession of pasture to forest in the Atlantic lowlands of Costa Rica. Global Biogeochem. Cycles 8 (4), 399–409. https://doi.org/10.1029/94GB01660.

Kemp, W.M., Boynton, W.R., Adolf, J.E., Boesch, D.F., Boicourt, W.C., Brush, G., Cornwell, J.C., Fisher, T.R., Glibert, P.M., Hagy, J.D., Harding, L.W., Houde, E.D., Kimmel, D.G., Miller, W.D., Newell, R.I.E., Roman, M.R., Smith, E.M., Stevenson, J. C., 2005. Eutrophication of Chesapeake Bay: historical trends and ecological interactions. Mar. Ecol. Prog. Ser. 303, 1–29. https://doi.org/10.3354/meps303001.

King, A.E., Choi, E., Burkhardt, J., Mueller, N.D., 2026. Soil organic carbon improves crop yield and yield resilience. Glob. Chang. Biol. 32 (5), e70909. https://doi.org/10.1111/gcb.70909.

Kjær, S.T., Lang, R., Kätterer, T., Dörsch, P., 2026. Species specific effects of cover crops on nitrous oxide emissions in hemiboreal cereal production: the importance of freeze-thaw driven emissions. Agr Ecosyst Environ 397, 110061. https://doi.org/10.1016/j.agee.2025.110061.

Künnemann, T., Cannavo, P., Guérin, V., Guénon, R., 2023. Soil CO_2, CH_4 and N_2O fluxes in open lawns, treed lawns and urban woodlands in Angers. France. Urban Ecosystems 26 (6), 1659–1672. https://doi.org/10.1007/s11252-023-01407-y.

Li, S., Xing, T., Sa, R., Zhang, Y., Chen, H., Jin, K., Shao, Q., Tang, S., Wang, C., 2024. Effects of grazing on soil respiration in global grassland ecosystems. Soil Tillage Res. 238, 106033. https://doi.org/10.1016/j.still.2024.106033.

Li, Z., Tang, Z., Song, Z., Chen, W., Tian, D., Tang, S., Wang, X., Wang, J., Liu, W., Wang, Y., Li, J., Jiang, L., Luo, Y., Niu, S., 2022. Variations and controlling factors of soil denitrification rate. Glob. Chang. Biol. 28 (6), 2133–2145. https://doi.org/10.1111/gcb.16066.

Lin, Q., Wu, Q., Chen, C., Lin, H., Xie, A., Jiang, C., Xia, X., 2025. Species-specific Effects of Litter Management on Soil Respiration Dynamics in Urban Green Spaces: Implications for Carbon Cycling and climate Regulation. Forests 16 (4). https://doi.org/10.3390/f16040642.

Livesley, S.J., Dougherty, B.J., Smith, A.J., Navaud, D., Wylie, L.J., Arndt, S.K., 2010. Soil-atmosphere exchange of carbon dioxide, methane and nitrous oxide in urban garden systems: impact of irrigation, fertiliser and mulch. Urban Ecosystems 13 (3), 273–293. https://doi.org/10.1007/s11252-009-0119-6.

Lu, C., Kotze, D.J., Setälä, H.M., 2022. Plant functional type affects nitrogen dynamics in urban park soils similarly to boreal forest soils. Plant and Soil 479 (1), 573–587. https://doi.org/10.1007/s11104-022-05544-9.

Luo, G.J., Kiese, R., Wolf, B., Butterbach-Bahl, K., 2013. Effects of soil temperature and moisture on methane uptake and nitrous oxide emissions across three different ecosystem types. Biogeosciences 10 (5), 3205–3219. https://doi.org/10.5194/bg-10-3205-2013.

MacDonald, J.A., Dise, N.B., Matzner, E., Armbruster, M., Gundersen, P., Forsius, M., 2002. Nitrogen input together with ecosystem nitrogen enrichment predict nitrate leaching from European forests. Glob. Chang. Biol. 8 (10), 1028–1033. https://doi.org/10.1046/j.1365-2486.2002.00532.x.

Maharjan, B., Venterea, R.T., Rosen, C., 2014. Fertilizer and Irrigation Management Effects on Nitrous Oxide Emissions and Nitrate Leaching. Agron. J. 106 (2), 703–714. https://doi.org/10.2134/agronj2013.0179.

Matson, P.A., Vitousek, P.M., Livingston, G.P., Swanberg, N.A., 1990. Sources of variation in nitrous oxide flux from amazonian ecosystems. J. Geophys. Res. Atmos. 95 (D10), 16789–16798. https://doi.org/10.1029/JD095iD10p16789.

Moyano, Fernando E., Manzoni, Stefano, Chenu, Claire, 2013. Responses of soil heterotrophic respiration to moisture availability: An exploration of processes and models. Soil Biology and Biochemistry 59, 72–85. https://doi.org/10.1016/j.soilbio.2013.01.002. https://linkinghub.elsevier.com/retrieve/pii/S0038071713000138.

Nielsen, O.-K., Plejdrup, M.S., Winther, M., Nielsen, M., Gyldenkærne, S, Mikkelsen, M. H., Albrektsen, R., Hjelgaard, K., Fauser, P., Bruun, H.G., Levin, L., Callisen, L.W.,

Andersen, T.A., Johannsen, V.K., Nord-Larsen, T., Vesterdal, L., Stupak, I., Scott-Bentsen, N., Rasmussen, E., Petersen, S.B., Baunbæk, L., Hansen, M.G., 2023. *Denmark's National Inventory Report 2023: Emission inventories 1990-2021 Submitted under the United Nations Framework Convention on climate Change*. Aarhus University, DCE – Danish Centre for Environment and Energy. https://dce2.au.dk/pub/SR541.pdf.

Nowak, D.J., Crane, D.E., Stevens, J.C., Hoehn, R.E., 2003. *The Urban Forest Effects (UFORE) Model: Field Data Collection Manual*. USDA Forest Service, Northeastern Research Station, Syracuse, NY, USA.

Paerl, H.W., Valdes, L.M., Peierls, B.L., Adolf, J.E., Harding, L.J.W., 2006. Anthropogenic and climatic influences on the eutrophication of large estuarine ecosystems. Limnol. Oceanogr. 51 (1part2), 448–462. https://doi.org/10.4319/lo.2006.51.1_part_2.0448.

Pan, B., Xia, L., Lam, S.K., Wang, E., Zhang, Y., Mosier, A., Chen, D., 2022. A global synthesis of soil denitrification: driving factors and mitigation strategies. Agr Ecosyst Environ 327. https://doi.org/10.1016/j.agee.2021.107850.

Paustian, K., Six, J., Elliott, E.T., Hunt, H.W., 2000. Management options for reducing CO_2 emissions from agricultural soils. Biogeochemistry 48 (1), 147–163. https://doi.org/10.1023/A:1006271331703.

Pelster, D.E., Thiagarajan, A., Liang, C., Chantigny, M.H., Wagner-Riddle, C., Congreves, K., Lemke, R., Glenn, A., Tenuta, M., Hernandez-Ramirez, G., Bittman, S., Hunt, D., Owens, J., MacDonald, D., 2022. Ratio of non-growing season to growing season N_2O emissions in Canadian croplands: an update to national inventory methodology. Can. J. Soil Sci. 103 (2), 344–352. https://doi.org/10.1139/cjss-2022-0101.

Phillips, R.L., McMillan, A.M.S., Palmada, T., Dando, J., Giltrap, D., 2014. Temperature effects on N_2O and N_2 denitrification end-products for a New Zealand pasture soil. N. Z. J. Agric. Res. 58 (1), 89–95. https://doi.org/10.1080/00288233.2014.969380.

Pouyat, R., Groffman, P., Yesilonis, I., Hernandez, L., 2002. Soil carbon pools and fluxes in urban ecosystems. Environ. Pollut. 116, S107–S118. https://doi.org/10.1016/S0269-7491(01)00263-9.

Qasim, W., Xia, L., Lin, S., Wan, L., Zhao, Y., Butterbach-Bahl, K., 2021. Global greenhouse vegetable production systems are hotspots of soil N_2O emissions and nitrogen leaching: a meta-analysis. Environ. Pollut. 272, 116372. https://doi.org/10.1016/j.envpol.2020.116372.

Ravishankara, A., Daniel, J.S., Portmann, R.W., 2009. Nitrous oxide (N_2O): the dominant ozone-depleting substance emitted in the 21st century. Science 326 (5949), 123–125. https://doi.org/10.1126/science.1176985.

Riches, D., Porter, I., Dingle, G., Gendall, A., Grover, S., 2020. Soil greenhouse gas emissions from Australian sports fields. Sci. Total Environ. 707, 134420. https://doi.org/10.1016/j.scitotenv.2019.134420.

Risk, N., Snider, D., Wagner-Riddle, C., 2013. Mechanisms leading to enhanced soil nitrous oxide fluxes induced by freeze–thaw cycles. Can. J. Soil Sci. 93 (4), 401–414. https://doi.org/10.4141/cjss2012-071.

Ruehlmann, J., 2020. Soil particle density as affected by soil texture and soil organic matter: 1. Partitioning of SOM in conceptional fractions and derivation of a variable SOC to SOM conversion factor. Geoderma 375, 114542. https://doi.org/10.1016/j.geoderma.2020.114542.

Schindlbacher, A., Zechmeister-Boltenstern, S., Butterbach-Bahl, K., 2004. Effects of soil moisture and temperature on NO, NO_2, and N_2O emissions from European forest soils. J. Geophys. Res. Atmos. 109 (D17). https://doi.org/10.1029/2004JD004590.

Seto, K.C., Güneralp, B., Hutyra, L.R., 2012. Global forecasts of urban expansion to 2030 and direct impacts on biodiversity and carbon pools. Proc. Natl. Acad. Sci. 109 (40), 16083–16088.

Shang, Z., Cui, X., van Groenigen, K.J., Kuhnert, M., Abdalla, M., Luo, J., Zhang, W., Song, Z., Jiang, Y., Smith, P., Zhou, F., 2024. Global cropland nitrous oxide emissions in fallow period are comparable to growing-season emissions. Glob. Chang. Biol. 30 (2), e17165. https://doi.org/10.1111/gcb.17165.

Sieczko, A.K., van de Vlasakker, P.C.H., Tonderski, K., Metson, G.S., 2023. Seasonal nitrogen and phosphorus leaching in urban agriculture: Dominance of non-growing season losses in a Southern swedish case study. Urban For. Urban Green. 79, 127823. https://doi.org/10.1016/j.ufug.2022.127823.

Smith, K.A., Ball, T., Conen, F., Dobbie, K.E., Massheder, J., Rey, A., 2018. Exchange of greenhouse gases between soil and atmosphere: interactions of soil physical factors and biological processes. Eur. J. Soil Sci. 69 (1), 10–20. https://doi.org/10.1111/ejss.12539.

Sousa, J.R., Cabral, F., Coutinho, J., 2016. Assessment of N Mineralization and N Leaching in Soil using a New in situ Incubation Method. Commun. Soil Sci. Plant Anal. 47 (19), 2157–2167. https://doi.org/10.1080/00103624.2016.1208751.

Statistics Denmark. (2025). AREALDK: Land by land cover, region and unit. StatBank Denmark. https://www.statbank.dk/AREALDK (accessed 20 May 2026).

Stefaner, K., Ghosh, S., Mohd Yusof, M.L., Ibrahim, H., Leitgeb, E., Schindlbacher, A., Kitzler, B., 2021. Soil greenhouse gas fluxes from a humid tropical forest and differently managed urban parkland in Singapore. Sci. Total Environ. 786, 147305. https://doi.org/10.1016/j.scitotenv.2021.147305.

Subke, J.-A., Bahn, M., 2010. On the 'temperature sensitivity' of soil respiration: can we use the immeasurable to predict the unknown? Soil Biol. Biochem. 42 (9), 1653–1656. https://doi.org/10.1016/j.soilbio.2010.05.026.

Telenko, D.E.P., Shaddox, T.W., Unruh, J.B., Trenholm, L.E., 2015. Nitrate Leaching, Turf Quality, and Growth Rate of 'Floratam' St. Augustinegrass and Common Centipedegrass. Crop Science 55 (3), 1320–1328. https://doi.org/10.2135/cropsci2014.09.0639.

Thompson, G.L., Kao-Kniffin, J., 2019. Urban Grassland Management Implications for Soil C and N Dynamics: a Microbial Perspective. Front. Ecol. Evol. 7. https://doi.org/10.3389/fevo.2019.00315.

Townsend-Small, A., Pataki, D.E., Czimczik, C.I., Tyler, S.C., 2011. Nitrous oxide emissions and isotopic composition in urban and agricultural systems in southern California. J. Geophys. Res. 116 (G1). https://doi.org/10.1029/2010jg001494.

Trémeau, J., Olascoaga, B., Backman, L., Karvinen, E., Vekuri, H., Kulmala, L., 2024. Lawns and meadows in urban green space – a comparison from perspectives of greenhouse gases, drought resilience and plant functional types. Biogeosciences 21 (4), 949–972. https://doi.org/10.5194/bg-21-949-2024.

Trenholm, L.E., Unruh, J.B., Sartain, J.B., 2012. Nitrate Leaching and Turf Quality in established 'Floratam' St. Augustinegrass and 'Empire' Zoysiagrass. J. Environ. Qual. 41 (3), 793–799. https://doi.org/10.2134/jeq2011.0183.

Trolove, S., Thomas, S., van der Klei, G., Beare, M., Cichota, R., Meenken, E., 2019. Nitrate leaching losses during pasture renewal – Effects of treading, urine, forages and tillage. Sci. Total Environ. 651, 1819–1829. https://doi.org/10.1016/j.scitotenv.2018.09.333.

United Nations, 2014. *World Urbanization Prospects: The 2014 Revision*, Highlights. United Nations, Department of Economic and Social Affairs, Population Division, New York. https://doi.org/10.18356/527e5125-en.

van Delden, L., Rowlings, D.W., Scheer, C., Grace, P.R., 2016. Urbanisation-related land use change from forest and pasture into turf grass modifies soil nitrogen cycling and increases N_2O emissions. Biogeosciences 13 (21), 6095–6106. https://doi.org/10.5194/bg-13-6095-2016.

Wagner-Riddle, C., Congreves, K.A., Abalos, D., Berg, A.A., Brown, S.E., Ambadan, J.T., Gao, X., Tenuta, M., 2017. Globally important nitrous oxide emissions from croplands induced by freeze–thaw cycles. Nat. Geosci. 10 (4), 279–283. https://doi.org/10.1038/ngeo2907.

Wagner-Riddle, C., Congreves, K.A., Brown, S.E., Helgason, W.D., Farrell, R.E., 2024. Overwinter and Spring Thaw Nitrous Oxide Fluxes in a Northern Prairie Cropland are Limited but a significant Proportion of Annual Emissions. Global Biogeochem. Cycles 38 (4), e2023GB008051. https://doi.org/10.1029/2023GB008051.

Walkiewicz, A., Bulak, P., Khalil, M.I., Osborne, B., 2025. Assessment of soil CO_2, CH_4, and N_2O fluxes and their drivers, and their contribution to the climate change mitigation potential of forest soils in the Lublin region of Poland. Eur. J. For. Res. 144 (1), 29–52. https://doi.org/10.1007/s10342-024-01739-0.

Wang, H., Gao, J.-E., Li, X.-H., Zhang, S.-L., Wang, H.-J., 2015. Nitrate accumulation and leaching in surface and ground water based on simulated rainfall experiments. PLoS One 10 (8), e0136274. https://doi.org/10.1371/journal.pone.0136274.

Wang, H., Li, Y., Zhang, J., Zhang, T., Wang, Y., Li, F.Y., 2025. Moderate grazing reduces while mowing increases greenhouse gas emissions from a steppe grassland: Key modulating function played by plant standing biomass. J. Environ. Manage. 374, 124142. https://doi.org/10.1016/j.jenvman.2025.124142.

Wang, Y., Feigenwinter, I., Hörtnagl, L., Gilgen, A.K., Buchmann, N., 2026. Drivers of long-term grassland CO_2 fluxes: effects of management and meteorological conditions during regrowth periods. Biogeosciences 23 (4), 1625–1652.

Wang, Y., Xiao, J., Ma, Y., Luo, Y., Hu, Z., Li, F., Li, Y., Gu, L., Li, Z., Yuan, L., 2021. Carbon fluxes and environmental controls across different alpine grassland types on the Tibetan Plateau. Agric. For. Meteorol. 311, 108694. https://doi.org/10.1016/j.agrformet.2021.108694.

Wangari, E.G., Mwanake, R.M., Houska, T., Kraus, D., Kikowatz, H.-M., Wolf, B., Gettel, G.M., Breuer, L., Ambus, P., Kiese, R., Butterbach-Bahl, K., 2024. Spatial-temporal patterns of foliar and bulk soil ^{15}N isotopic signatures across a heterogeneous landscape: Linkages to soil N status, nitrate leaching, and N_2O fluxes. Soil Biol. Biochem. 199. https://doi.org/10.1016/j.soilbio.2024.109609.

WHO. (2010). Urban planning, environment and health: From evidence to policy action. WHO Regional Office for Europe.

Wolf, B., Zheng, X., Brüggemann, N., Chen, W., Dannenmann, M., Han, X., Sutton, M.A., Wu, H., Yao, Z., Butterbach-Bahl, K., 2010. Grazing-induced reduction of natural nitrous oxide release from continental steppe. Nature 464 (7290), 881–884. https://doi.org/10.1038/nature08931.

Woodward, E., Raij-Hoffman, I., Scow, K., Tautges, N., 2022. Alfalfa reduces winter nitrate leaching relative to organic and conventional annual vegetable systems: Resin bag field measurements and modeling with HYDRUS-1D. J. Soil Water Conserv. 77 (5), 450–465. https://doi.org/10.2489/jswc.2022.00155.

Wu, X., Brüggemann, N., Gasche, R., Shen, Z., Wolf, B., Butterbach-Bahl, K., 2010. Environmental controls over soil-atmosphere exchange of N_2O, NO, and CO_2 in a temperate Norway spruce forest. Global Biogeochem. Cycles 24 (2). https://doi.org/10.1029/2009GB003616.

Wyland, L.J., Jackson, L.E., 1993. Evaluating Nitrate Recovery by Ion-Exchange Resin Bags. Soil Sci. Soc. Am. J. 57 (5), 1208–1211. https://doi.org/10.2136/sssaj1993.03615995005700050008x.

Xie, J., Zhan, Y., Li, X., Dai, Z., Cong, R., Xu, R., Zhang, Z., Yao, Z., 2025. Significant carbon storage and sequestration by urban greenery in Beijing city during 2010–2020. Urban For. Urban Green. 112, 128944. https://doi.org/10.1016/j.ufug.2025.128944.

Xu, X., Tian, H., Hui, D., 2008. Convergence in the relationship of CO_2 and N_2O exchanges between soil and atmosphere within terrestrial ecosystems. Glob. Chang. Biol. 14 (7), 1651–1660. https://doi.org/10.1111/j.1365-2486.2008.01595.x.

Yan, R., Zhang, Y., Wang, M., Li, R., Jin, D., Xin, X., Li, L., 2021. Interannual variation in ecosystem respiration in an Inner Mongolian meadow steppe in response to livestock grazing. Ecol. Ind. 131, 108121. https://doi.org/10.1016/j.ecolind.2021.108121.

Yao, Z., Guo, H., Wang, Y., Zhan, Y., Zhang, T., Wang, R., Zheng, X., Butterbach-Bahl, K., 2024. A global meta-analysis of yield-scaled N_2O emissions and its mitigation efforts for maize, wheat, and rice. Glob. Chang. Biol. 30 (2), e17177. https://doi.org/10.1111/gcb.17177.

Yao, Z., Pelster, D.E., Liu, C., Zheng, X., Butterbach-Bahl, K., 2020. Soil N intensity as a measure to estimate annual N_2O and NO fluxes from natural and managed

ecosystems. Curr. Opin. Environ. Sustain. 47, 1–6. https://doi.org/10.1016/j.cosust.2020.03.008.

Yao, Z., Wang, R., Zhang, H., Ma, L., Zheng, X., Liu, C., Zhang, W., Wang, Y., Zhu, B., Butterbach-Bahl, K., 2025. Rodent-induced grassland degradation increases annual non-CO_2 greenhouse gas fluxes and NO losses despite CH_4 uptake enhancement. Agric. For. Meteorol. 368, 110534. https://doi.org/10.1016/j.agrformet.2025.110534.

Yao, Z., Wu, X., Wolf, B., Dannenmann, M., Butterbach-Bahl, K., Brüggemann, N., Chen, W., Zheng, X., 2010. Soil-atmosphere exchange potential of NO and N_2O in different land use types of Inner Mongolia as affected by soil temperature, soil moisture, freeze-thaw, and drying-wetting events. J. Geophys. Res. Atmos. 115 (D17). https://doi.org/10.1029/2009JD013528.

Yu, H., Duan, Y., Mulder, J., Dörsch, P., Zhu, W., Xu, R., Huang, K., Zheng, Z., Kang, R., Wang, C., Quan, Z., Zhu, F., Liu, D., Peng, S., Han, S., Zhang, Y., Fang, Y., 2023. Universal temperature sensitivity of denitrification nitrogen losses in forest soils. Nat. Clim. Chang. 13 (7), 726–734. https://doi.org/10.1038/s41558-023-01708-2.

Yu, L., Zhang, Q., Tian, Y., Sun, W., Scheer, C., Li, T., Zhang, W., 2022. Global variations and drivers of nitrous oxide emissions from forests and grasslands. Front. Soil Sci. 2–2022. https://doi.org/10.3389/fsoil.2022.1094177.

Zhan, Y., Xie, J., Yao, Z., Wang, R., He, X., Wang, Y., Zheng, X., 2021. Characteristics of annual N_2O and NO fluxes from chinese urban turfgrasses. Environ. Pollut. 290, 118017. https://doi.org/10.1016/j.envpol.2021.118017.

Zhan, Y., Yao, Z., Groffman, P.M., Xie, J., Wang, Y., Li, G., Zheng, X., Butterbach-Bahl, K., 2023. Urbanization can accelerate climate change by increasing soil NO_2 emission while reducing CH_4 uptake. Glob. Chang. Biol. 29 (12), 3489–3502. https://doi.org/10.1111/gcb.16652.

Zhang, H., Yao, X., Zeng, W., Fang, Y., Wang, W., 2020. Depth dependence of temperature sensitivity of soil carbon dioxide, nitrous oxide and methane emissions. Soil Biol. Biochem. 149. https://doi.org/10.1016/j.soilbio.2020.107956.

Zhang, J., Peng, C., Zhu, Q., Xue, W., Shen, Y., Yang, Y., Shi, G., Shi, S., Wang, M., 2016. Temperature sensitivity of soil carbon dioxide and nitrous oxide emissions in mountain forest and meadow ecosystems in China. Atmos. Environ. 142, 340–350. https://doi.org/10.1016/j.atmosenv.2016.08.011.

Zhang, T., Wang, G., Yang, Y., Mao, T., Chen, X., 2017. Grassland types and season-dependent response of ecosystem respiration to experimental warming in a permafrost region in the Tibetan Plateau. Agric. For. Meteorol. 247, 271–279. https://doi.org/10.1016/j.agrformet.2017.08.010.

Zhou, M., Zhu, B., Butterbach-Bahl, K., Zheng, X., Wang, T., Wang, Y., 2013. Nitrous oxide emissions and nitrate leaching from a rain-fed wheat-maize rotation in the Sichuan Basin, China. Plant and Soil 362 (1), 149–159. https://doi.org/10.1007/s11104-012-1269-5.

Zhu, W.-X., Dillard, N.D., Grimm, N.B., 2005. Urban nitrogen biogeochemistry: status and processes in green retention basins. Biogeochemistry 71 (2), 177–196. https://doi.org/10.1007/s10533-005-0683-7.